A block minimum residual norm subspace solver for sequences of multiple left and right-hand side linear systems

Luc Giraud, Yan-Fei Jing, Yanfei Xiang

A block minimum residual norm subspace solver for sequences of multiple left and right-hand side linear systems

L. Giraud, Y.-F. Jing, Y.-F. Xiang

RESEARCH REPORT
N° 9393
February 2021
Project-Teams HiePACS

ISSN 0249-6399 ISRN INRIA/RR--9393--FR+ENG

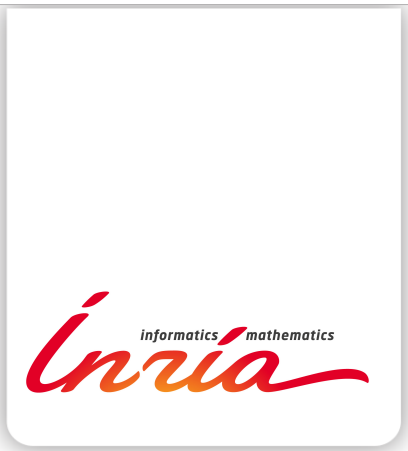

A block minimum residual norm subspace solver for sequences of multiple left and right-hand side linear systems

L. Giraud*, Y.-F. Jing†, Y.-F. Xiang* ‡

Project-Teams HiePACS

Research Report n° 9393 — February 2021 — 50 pages

Abstract: We are concerned with the iterative solution of linear systems with multiple right-hand sides available one group after another, including the case where there are massive number (like tens of thousands) of right-hand sides associated with a single matrix so that all of them cannot be solved at once but rather need to be split into chunks of possible variable sizes. For such sequences of linear systems with multiple left and right-hand sides, we develop a new recycling block generalized conjugate residual method with inner orthogonalization and inexact breakdown (IB-BGCRO-DR), which glues subspace recycling technique in GCRO-DR [SIAM J. Sci. Comput., 28(5) (2006), pp. 1651–1674] and inexact breakdown mechanism in IB-BGMRES [Linear Algebra Appl., 419 (2006), pp. 265–285] to guarantee this new algorithm could reuse spectral information for subsequent cycles as well as for the remaining linear systems to be solved. Related variant IB-BFGCRO-DR that suits for flexible preconditioning is devised to cope with constraints on some applications while also enabling mixed-precision calculation, which provides advantages in speed and memory usage over double precision as well as in perspective of emerging computing units such as the GPUs.

Key-words: Block subspace methods, augmentation, deflation, subspace recycling, Block-GMRES, inexact block rank deficiency.

* Inria, France

† School of Mathematical Sciences/Institute of Computational Science, University of Electronic Science and Technology of China, Chengdu, Sichuan, 611731, P. R. China - supported by Science Challenge Project (TZ2016002-TZZT2019-B1.4), NSFC (12071062, 61772003), Key Projects of Applied Basic Research in Sichuan Province (Grant No. 2020YJ0216), and Science Strength Promotion Programme of UESTC.

‡ Cerfacs, France

RESEARCH CENTRE
BORDEAUX – SUD-OUEST

200 avenue de la Vieille Tour
33405 Talence Cedex

Une méthode bloc de sous-espace minimisant la norme des résidus pour des séquence de systèmes linéaires

Résumé : Nous nous intéressons à la solution itérative de systèmes linéaires avec plusieurs second-membres disponibles un groupe après l'autre, y compris le cas où il y a un nombre massif (comme des dizaines de milliers) de second-membres associés à une seule matrice de sorte que tous ne peuvent pas être résolus en une fois mais doivent plutôt être divisés en morceaux de tailles variables possibles. Pour de telles séquences de systèmes linéaires à matrices et second-membres multiples, nous développons une nouvelle méthode de recyclage des résidus conjugués généralisés par blocs avec orthogonalisation interne et convergence partielle (IB-BGCRO-DR), qui exploite technique de recyclage subspatial dans GCRO-DR [SIAM J. Sci. Comput., 28(5) (2006), pp. 1651-1674] mécanisme de convergence partielle dans IB-BGMRES [Algèbre linéaire, 419 (2006), pp. 265-285] pour garantir que ce nouvel algorithme pourrait réutiliser les informations spectrales pour les cycles suivants ainsi que pour les systèmes linéaires restants à résoudre. La variante connexe IB-BFGCRO-DR qui convient au préconditionnement flexible est conçue pour faire face aux contraintes de certaines applications tout en permettant un calcul de précision mixte, ce qui présente des avantages en termes de vitesse et d'utilisation de la mémoire par rapport à la double précision ainsi que dans la perspective des unités de calcul émergentes telles que les GPU. En outre, nous discutons également des choix possibles lors de la construction d'un sous-espace de recyclage ainsi que de la manière d'exploiter le mécanisme de convergence partielle pour réaliser la flexibilité des politiques d'expansion de l'espace de recherche et surveiller les seuils de convergence individuels pour chaque second-membre. Comme effet secondaire, on peut également illustrer le fait que cette méthode peut être appliquée au cas des matrices constantes ou variant lentement. Enfin, nous démontrons les avantages numériques et informatiques de la combinaison de ces idées dans de tels algorithmes sur un ensemble d'exemples académiques simples.

Mots-clés : Méthode bloc de sous-espace, augmentation, déflation, recyclage de sous-espace, block-GMRES, convergence partielle.

Contents

1 Introduction

Many scientific and industrial simulations require the solution of a sequence of linear systems with multiple right-hand sides and possibly slowly-changing left-hand sides. In that context, one has to solve a series of linear systems of the form

$$A^{(\ell)}X^{(\ell)} = B^{(\ell)}, \quad \ell = 1, 2, \ldots, \tag{1}$$

where, associated with the ℓ^{th} family, $A^{(\ell)} \in \mathbb{C}^{n\times n}$ is a square nonsingular matrix of large dimension n along the family index ℓ, $B^{(\ell)} = [b^{(\ell,1)}, b^{(\ell,2)}, \ldots, b^{(\ell,p^{(\ell)})}] \in \mathbb{C}^{n\times p^{(\ell)}}$ are simultaneously given right-hand sides of full rank with $p^{(\ell)} \ll n$, and $X^{(\ell)} = [x^{(\ell,1)}, x^{(\ell,2)}, \ldots, x^{(\ell,p^{(\ell)})}] \in \mathbb{C}^{n\times p^{(\ell)}}$ are the solutions to be computed. Both the coefficient matrix $A^{(\ell)}$ and right-hand sides $B^{(\ell)}$ change from one family to the next, and the families of linear systems are typically available in sequence.

When solving sequences of linear systems as Equation (1), attractive approaches are those that can exploit information generated during the solution of a given system to accelerate the convergence for the next ones. Deflated restarting implements a similar idea between the cycles in the generalized minimum residual norm method (GMRES) [18, 21, 27]; it is realized by using a deflation subspace containing a few approximate eigenvectors deemed to hamper the convergence of the Krylov subspace methods [10–12]. Another alternative technique is the subspace recycling strategy proposed in the generalized conjugate residual method with inner orthogonalization (GCRO) and deflated restarting (GCRO-DR) method [15]. This latter method can reuse information accumulated in previous cycles as well as that accumulated in previous families. Given the multiple right-hand sides of Equation (1) are simultaneously available, block Krylov subspace methods are often considered as the suitable candidates for their capability of sharing search subspace that can be generated using basic linear algebra subprograms, level 3, (BLAS3)-like implementation [9]. A common issue in block Krylov subspace methods is the rank deficiency that might appear when expanding the residual spaces, which is caused by the convergence of individual or linear combination of solution vectors. Such rank deficiency problem could lead the block Arnoldi process to break down before the solutions for all the right-hand sides are found. For the sake of balancing robustness and convergence rate, Robbé and Sadkane proposed an inexact breakdown detecting mechanism for the block GMRES algorithm (denoted by IB-BGMRES) [19], which could keep and reintroduce directions associated with the almost converged parts in next iteration if necessary. We refer to [1, 2, 19] for relevant works on inexact breakdown detection, as well as to [23–26, 28] for related variants of block Krylov subspace methods for solving linear systems with multiple right-hand sides.

The contribution of this paper is twofold. We first show how to combine subspace recycling techniques of GCRO-DR [15] for recycling spectral information at a new cycle/family with the inexact breakdown mechanism introduced by Robbé and Sadkane in IB-BGMRES [19] for handling the issue of almost rank deficient block generated by the block Arnoldi procedure to develop the IB-BGCRO-DR algorithm, a new recycling block GCRO-DR variant with inexact breakdown detection. This is a natural extension of our previous work IB-BGMRES-DR [1], that enables the deflated restarting strategy proposed by Morgan [12] to be applied not only at restart but also when solving a sequence of linear systems; the IB-BGCRO-DR can reuse spectral information both from the solutions of previous cycle and family thus showing obvious advantages when solving sequences of linear systems like Equation (1). The second contribution is related to the block search space expansion policies that can be further developed based on the inexact breakdown mechanism. In particular, for stopping criterion based on backward error we introduce new strategies enabling to focus on the computational effort while ensuring the final accuracy of each individual solution.

The remainder of this paper is organized as follows. Section 2 is devoted to the development of the new algorithm, it contains some background parts that enable us to introduce the various numerical ingredients and notations required to design our algorithm. In Section 2.1 we first recall the governing ideas of the minimum norm residual Krylov method GCRO in a single right-hand side setting and briefly

present its block variant in Section 2.2. Next in Section 2.3 we present how the original inexact breakdown mechanism [19] introduced for block GMRES can be applied to block GCRO as well. These two main ingredients are combined to develop the new algorithm IB-BGCRO-DR in Section 2.4 and its flexible preconditioning variant referred to as IB-BFGCRO-DR discussed in Section 2.5. In Section 3, we describe how to extend the original inexact breakdown mechanism to best adapt the computational effort and reach the targeted accuracy prescribed by the stopping criterion in terms of backward errors for the individual solutions. In particular, we derive strategies to manage the situation where the individual right-hand sides need to be solved with different convergence thresholds. We also present policies adapted to stopping criterion based on normwise backward error on the right-hand side only (i.e. classical residual norm scaled by the norm of the right-hand side) or the more general one used to establish the backward stability of GMRES [13]. In Section 4, some remarks on computational and algorithmic aspects are detailed; the associated pseudocode of the IB-BGCRO-DR algorithm is presented as well. In Section 5 we present numerical experiments that illustrate the benefits of the new algorithm with both constant and slowly varying successive linear systems with multiple right-hand sides as well as the numerical capabilities of the novel search space expansion policies. Finally some concluding remarks are detailed in Section 6.

The symbol $||\cdot||$ denotes the Euclidean norm defaultly for both vectors and matrices, and the Frobenius norm is denoted with the subscript $_F$. The superscript ^{H} denotes the transpose conjugate and ^{T} for transpose. Because many notations are involved, we make choices to help the readability of the paper. The vectors are described by lowercase letter, matrices with multiple columns described by uppercase letter, the calligraphy uppercase letters like $\mathscr{V}$ represent the matrices whose columns are enlarged by multiple columns at each iteration as commonly appearing in the block Krylov context, and the uppercase letter with blackboard bold form like $\mathbb{V}$ refers to the block Krylov basis generated at each iteration. The superscript † refers to the Moore-Penrose inverse and other superscripts with different contents are also employed in main context for target illustrations, which will be explained when it locally appears thus we omit here. For convenience of the algorithm illustration and presentation, some MATLAB notations are used. Without special note, a subscript $_j$ for a vector (in single right-hand case) or a matrix (in block case) is used to indicate that the vector or matrix is obtained at iteration j and the positive subscript integer $_m$ represents the maximal iteration number of each (block) Krylov cycle. All the involved recycling subspaces of dimension k are described as a matrix with the subscript $_k$ whose columns form a basis. A matrix $C \in \mathbb{C}^{m\times\ell}$ consisting of m rows and ℓ columns sometimes is denoted as $C_{m\times\ell}$ explicitly. The identity and null matrices of dimension m are denoted respectively by I_m and 0_m or just I and 0 when the dimension is evident from the context. If $C \in \mathbb{C}^{m\times\ell}$, the singular values of C are denoted by $\sigma_1(C) \geq \ldots \geq \sigma_{min(m,\ell)}(C)$ in descent order; furthermore we denote span(C) the space spanned by the columns of C.

For simplicity and notational convenience, we drop in the rest of this paper the superscript $^{(\ell)}$ in $B^{(\ell)}$ and $X^{(\ell)}$ when considering to solve the current ℓ^{th} family of linear systems in the entire sequence of families. We indicate the superscript for a family order explicitly when necessary. That is, suppose that the current ℓ^{th} family of linear systems to be solved is

$$AX = B, \tag{2}$$

where, $A \in \mathbb{C}^{n\times n}$ is the current square nonsingular matrix of dimension n, $B = [b^{(1)}, b^{(2)}, \ldots, b^{(p)}] \in \mathbb{C}^{n\times p}$ are the simultaneously given right-hand sides and $X = [x^{(1)}, x^{(2)}, \ldots, x^{(p)}] \in \mathbb{C}^{n\times p}$ are the solutions to be computed.

2 Block GCRO-DR with inexact breakdown

For the sake of completeness of the exposure, this section contains some possibly well-known background which enables us to introduce the numerous notations required to describe the new algorithm

and detail its properties. In that respect, we first recall the main ingredients of the subspace recycling techniques existing in the minimum residual Krylov methods GCRO [6] and GCRO-DR [15] that are presented in the single right-hand side context. The straightforward extension to the multiple right-hand sides framework, that is the block formulation of GCRO-DR (BGCRO-DR) [14,16,17] is next introduced. Then the driving ideas of inexact breakdown mechanism [19] as well as the corresponding block Arnoldi-like recurrence equation are derived in the block GCRO-DR context leading to the new IB-BGCRO-DR algorithm.

2.1 GCRO

The background of GCRO [6] is briefly reviewed first in the case of a single right-hand side and then extended to the block case. The GCRO method relies on a given full-rank matrix $U_k \in \mathbb{C}^{n\times k}$, and a matrix C_k as the image of U_k by A satisfying the relations

$$AU_k = C_k, \tag{3}$$
$$C_k^H C_k = I_k. \tag{4}$$

For the solution of a single right-hand side linear system $Ax = b$ and a given initial guess x_0, the governing idea is to first define $x_1 \in x_0 + \mathrm{Range}(U_k)$ that minimizes the residual norm. From x_1 and its associated residual r_1, Arnoldi iterations are performed to enlarge the nested orthonormal basis of the residual spaces. The vector

$$x_1 = \underset{x\in x_0+\mathrm{Range}(U_k)}{\mathrm{argmin}} ||b - Ax||,$$

is defined by

$$x_1 = x_0 + U_k C_k^H r_0, \text{ and } r_1 = (I - C_k C_k^H) r_0 \text{ so that } r_1 \in C_k^{\perp}.$$

Starting from the unitary vector $v_1 = r_1/\|r_1\|$, the Arnoldi procedure enables us to form an orthonormal basis $V_m = [v_1, ..., v_m]$ of the Krylov space $\mathcal{K}_m((I-C_kC_k^H)A, v_1) = \mathrm{span}(v_1, (I-C_kC_k^H)Av_1, ..., ((I-C_kC_k^H)A)^{m-1}v_1)$ that can be written in the matrix form as

$$(I - C_k C_k^H)AV_m = V_{m+1}\underline{H}_m, \tag{5}$$

where $\underline{H}_m \in \mathbb{C}^{(m+1)\times m}$ is a Hessenberg matrix. Combining Equation (3) and (5) in a matrix form allows us to write a relation very similar to an Arnoldi equality that reads

$$A\widehat{W}_m = \widehat{V}_{m+1}\underline{G}_m,$$

where $\widehat{W}_m = [U_k, V_m]$ defines a basis of the search space, $\widehat{V}_{m+1} = [\, C_k, V_{m+1}]$ is an orthonomal basis of the residual space and $\underline{G}_m = \begin{bmatrix} I_k & B_m \\ 0_{(m+1)\times k} & \underline{H}_m \end{bmatrix} \in \mathbb{C}^{(k+m+1)\times(k+m)}$ with $\widehat{V}_{m+1}^H\widehat{V}_{m+1} = I_{m+1}$ and $B_m = C_k^H AV_m$. The minimum residual norm solution in the affine space $x_1 + \mathrm{Range}(\widehat{W}_m)$ can be written as $x_m = x_1 + \widehat{W}_m y_m$ where

$$y_m = \underset{y\in\mathbb{C}^{k+m}}{\mathrm{argmin}} \|c - \underline{G}_m y\|$$

and $c = \widehat{V}_{m+1}^H r_1 = (0_k, \|r_1\|, 0_m)^T \in \mathbb{C}^{k+m+1}$ are the components of the residual associated with x_1 in the residual space spanned by the columns of $\widehat{V}_{m+1}$.

GCRO and GMRES [21], both belong to the family of residual norm minimization approaches and rely on an orthonormal basis of the residual space. In addition to sharing the Arnoldi procedure to form part of or all this basis, they do also share the property of "happy breakdown"; that is, if the search space

cannot be enlarged because the new direction computed by the Arnoldi process is the null vector, then the solution is exactly found in the search space. This sharing of features does extend to the block context for the solution of linear system with multiple right-hand sides; in particular the inexact breakdown principle introduced in [19] in the context of block GMRES can be extended to block GCRO as discussed in the sequel. The purpose of the inexact breakdown mechanism is to prevent in an elegant and effective way the loss of numerical rank of the search space basis, that turns out to be also a way to monitor the search space extension according to the final target accuracy.

2.2 Block GCRO

The straightforward extension of the GCRO method in the block context is briefly described below. To facilitate reading, we change the calligraphy of the notation but keep the same letters to denote the block counterpart of the quantities involved in the method. Starting from the block initial guess $X_0 = [x_0^{(1)}, x_0^{(2)}, \ldots, x_0^{(p)}] \in \mathbb{C}^{n\times p}$ and associated initial residual block $R_0 = B - AX_0$, one can define

$$X_1 = \underset{X\in X_0+\mathrm{Range}(U_k)}{\mathrm{argmin}} ||B - AX||_F,$$

given by

$$X_1 = X_0 + U_k C_k^H R_0 \text{ and } R_1 = (I - C_k C_k^H)R_0 \text{ such that } R_1 \in C_k^{\perp}. \tag{6}$$

For the sake of simplicity of exposure, we first assume that R_1 is of full rank and denote $R_1 = \mathbb{V}_1\Lambda_1$ as its reduced QR-factorization. The orthonormal block $\mathbb{V}_1$ is then used to build the search space via m steps of block Arnoldi procedure depicted in Algorithm 1 to generate $\mathscr{V}_m = [\mathbb{V}_1, ..., \mathbb{V}_m]$ whose columns form an orthonormal basis of $\mathcal{K}_m((I - C_k C_k^H)A, \mathbb{V}_1) = \bigoplus_{t=1}^{p} \mathcal{K}_m((I - C_k C_k^H)A, v_1^{(t)})$. The block

Algorithm 1 *Block Arnoldi procedure with deflation of the C_k space*

1: Given a nonsingular coefficient matrix $A \in \mathbb{C}^{n\times n}$, choose an unitary matrix $\mathbb{V}_1$ of size $n \times p$
2: **for** $j = 1, 2, \ldots, m$ **do**
3: Compute $\mathbb{W}_j = (I - C_k C_k^H)A\mathbb{V}_j$
4: **for** $i = 1, 2, \ldots, j$ **do**
5: $H_{i,j} = \mathbb{V}_i^H \mathbb{W}_j$
6: $\mathbb{W}_j = \mathbb{W}_j - \mathbb{V}_i H_{i,j}$
7: **end for**
8: $\mathbb{W}_j = \mathbb{V}_{j+1} H_{j+1,j}$ (reduced QR-factorization of $\mathbb{W}_j$)
9: **end for**

Arnoldi procedure leads to the matrix equality

$$(I - C_k C_k^H)A\mathscr{V}_m = \mathscr{V}_{m+1}\underline{\mathscr{H}}_m, \tag{7}$$

where $\underline{\mathscr{H}}_m$ is a block Hessenberg matrix with (i, j) block defined by $H_{i,j}$. Similarly to the single right-hand side case, Equation (3) and (7) can be gathered in a matrix form

$$A\widehat{\mathscr{W}}_m = \widehat{\mathscr{V}}_{m+1}\underline{\mathcal{G}}_m, \tag{8}$$

where $\widehat{\mathscr{W}}_m = [U_k, \mathscr{V}_m] \in \mathbb{C}^{n\times(k+mp)}$, $\widehat{\mathscr{V}}_{m+1} = [C_k, \mathscr{V}_{m+1}] \in \mathbb{C}^{n\times(k+(m+1)p)}$ and $\underline{\mathcal{G}}_m = \begin{bmatrix} I_k & \mathcal{B}_m \\ 0_{(m+1)p\times k} & \underline{\mathscr{H}}_m \end{bmatrix} = \begin{bmatrix} \mathcal{G}_m & \\ 0_{p\times(k+(m-1)p)} & H_{m+1,m} \end{bmatrix} \in \mathbb{C}^{(k+(m+1)p)\times(k+mp)}$ with $\widehat{\mathscr{V}}_{m+1}^H\widehat{\mathscr{V}}_{m+1} = I_{(m+1)\times p}$ and $\mathcal{B}_m =$

$C_k^H A\mathscr{V}_m \in \mathbb{C}^{k\times mp}$ with $mp = m \times p$. The minimum residual norm solution in the affine space $X_1 + \mathrm{Range}(\widehat{W}_m)$ can be written as $X_m = X_1 + \widehat{\mathscr{W}_m} Y_m$ where

$$Y_m = \underset{Y\in\mathbb{C}^{(k+mp)\times p}}{\operatorname{argmin}} \|\mathcal{C} - \underline{\mathcal{G}}_m Y\|_F,$$

$\mathcal{C} = \mathscr{V}_{m+1}^H R_1 = (0_{k\times p}, \Lambda_1^T, 0_{mp\times p})^T \in \mathbb{C}^{(k+(m+1)p)\times p}$ and the columns of $\mathcal{C}$ are the components of the initial residual block R_1 in the residual space $\mathscr{V}_{m+1}$.

2.3 Block GCRO with inexact breakdowns

When one solution or a linear combination of the solutions has converged, the block-Arnoldi procedure implemented to build an orthonormal basis of $\mathcal{K}_j((I - C_k C_k^H)A, \mathbb{V}_1)$ needs to be modified to account for this partial convergence. This partial convergence is characterized by a numerical rank deficiency in the new p directions that are usually introduced for enlarging the search space at the next iteration. In [19], the authors present an elegant numerical variant that enables the detection of what is referred to as inexact breakdowns. In that approach the directions that have a low contribution to the residual block are discarded from the set of vectors used to expand the search space at the next iteration, but these abandoned directions are kept and reintroduced in iterations afterwards if necessary. In this section, we try to give an insight and the main equality required to derive the IB-BGCRO-DR algorithm. We refer the reader to the original paper [19] for a detailed and complete description. For the sake of simplicity of exposure and easy cross-reading, we adopt most of the notations from [1, 19].

Because when an inexact breakdown occurs, not all the space spanned by $\mathbb{W}_j$ is considered to build $\mathbb{V}_{j+1}$ in order to expand the search space. For the sake of simplicity, we assume that $p_1 = p$ and we denote by p_{j+1} the number of columns of the block orthonormal basis vector $\mathbb{V}_{j+1}$. Then $\mathbb{V}_{j+1} \in \mathbb{C}^{n\times p_{j+1}}, \mathbb{W}_j \in \mathbb{C}^{n\times p_j}$ and $H_{j+1,j} \in \mathbb{C}^{p_{j+1}\times p_j}$. As a consequence the dimension of the search space $\mathcal{K}_j((I - C_k C_k^H)A, \mathbb{V}_1)$ considered at the j^{th} iteration is no longer necessarily equal to $j \times p$ but is equal to $n_j = \sum_{i=1}^{j} p_i$; that is, the sum of the column rank of $\mathbb{V}_i's$ $(i = 1, \ldots, j)$.

When no inexact breakdown has occurred $p_{j+1} = p_j = \ldots = p_1 = p$, the range of $\mathbb{W}_j$ has always been used to enlarge the search space and we obtain the block relation given by Equation (8). To account for a numerical deficiency in the residual block $R_j = B - AX_j$ in a way that is described later, Robbé and Sadkane [19] proposed to split

$$\mathbb{W}_j = \mathbb{V}_{j+1} H_{j+1,j} + Q_j \tag{9}$$

so that the columns of Q_j and $\mathbb{V}_{j+1}$ are orthogonal to each other and only $\mathbb{V}_{j+1}$ is used to enlarge $\mathscr{V}_j$ to form $\mathscr{V}_{j+1}$. We can then extend Equation (8) into

$$A\widehat{\mathscr{W}_j} = \widehat{\mathscr{V}_j}\mathcal{G}_j + [0_{n\times k},\ \mathcal{Q}_{j-1},\ \mathbb{W}_j], \tag{10}$$

where $\mathcal{G}_j \in \mathbb{C}^{(k+n_j)\times(k+n_j)}$ is the first $k+n_j$ rows of $\underline{\mathcal{G}}_j \in \mathbb{C}^{(k+n_j+p)\times(k+n_j)}$, $\mathcal{Q}_{j-1} = [Q_1, \ldots, Q_{j-1}] \in \mathbb{C}^{n\times n_{j-1}}$ accounts for all the abandoned directions. The matrix $\mathcal{Q}_{j-1}$ is rank deficient, and it reduces to the zero matrix of $\mathbb{C}^{n\times n_{j-1}}$ as long as no inexact breakdown has occurred.

In order to characterize a minimum norm solution in the space spanned by $\widehat{\mathscr{W}_j}$ using Equation (10) we need to form an orthonormal basis of the space spanned by $[\widehat{\mathscr{V}_j}, \mathcal{Q}_{j-1}, \mathbb{W}_j]$. This is performed by first orthogonalizing $\mathcal{Q}_{j-1}$ against $\widehat{\mathscr{V}_j}$, that is $\widetilde{\mathcal{Q}}_{j-1} = (I - \widehat{\mathscr{V}_j}\widehat{\mathscr{V}_j}^H)\mathcal{Q}_{j-1}$. Because $\mathcal{Q}_{j-1}$ is of low rank so is $\widetilde{\mathcal{Q}}_{j-1}$ that can be written

$$\widetilde{\mathcal{Q}}_{j-1} = P_{j-1}\mathbb{G}_{j-1} \text{ with } \begin{cases} P_{j-1} \in \mathbb{C}^{n\times q_j} \text{ has orthonormal columns with } \widehat{\mathscr{V}_j}^H P_{j-1} = 0, \\ \mathbb{G}_{j-1} \in \mathbb{C}^{q_j\times n_{j-1}} \text{ is of full rank with } q_j = p - p_j. \end{cases} \tag{11}$$

Next $\mathbb{W}_j$, that is already orthogonal to $\widehat{\mathscr{V}_j}$, is made to be orthogonal to P_{j-1} with $\mathbb{W}_j - P_{j-1}E_j$ where $E_j = P_{j-1}^H \mathbb{W}_j$; then one computes $\widetilde{W}_j D_j$ with $\widetilde{W}_j \in \mathbb{C}^{n\times p_j}$ and $D_j \in \mathbb{C}^{p_j\times p_j}$ by carrying out the reduced QR-factorization of the tall and skinny matrix $\mathbb{W}_j - P_{j-1}E_j$. Eventually, the columns of the matrix $[\widehat{\mathscr{V}_j}, P_{j-1}, \widetilde{W}_j]$ form an orthonormal basis of the residual space spanned by $[\widehat{\mathscr{V}_j}, \mathcal{Q}_{j-1}, \mathbb{W}_j]$.

With this new basis, Equation (10) writes

$$\begin{aligned} A[U_k, \mathscr{V}_j] = \; & [C_k, \mathscr{V}_j] \begin{bmatrix} I & \mathcal{B}_j \\ 0 & \mathscr{L}_j \end{bmatrix} + \left[0_k, P_{j-1}\mathbb{G}_{j-1}, \left[P_{j-1}, \widetilde{W}_j\right] \begin{bmatrix} E_j \\ D_j \end{bmatrix}\right] \\ = \; & \left[C_k, \mathscr{V}_j, P_{j-1}, \widetilde{W}_j\right] \begin{bmatrix} I_k & & \mathcal{B}_j \\ & & \mathscr{L}_j \\ 0_{(n_j+p)\times k} & \mathbb{G}_{j-1} & E_j \\ & 0 & D_j \end{bmatrix}, \end{aligned} \tag{12}$$

where $\mathscr{L}_j = \begin{bmatrix} H_{1,1} & H_{1,2} & H_{1,3} & \cdots & H_{1,j} \\ H_{2,1} & H_{2,2} & H_{2,3} & \cdots & H_{2,j} \\ \mathbb{V}_3^H Q_1 & H_{3,2} & H_{3,3} & \cdots & H_{3,j} \\ \vdots & \vdots & \vdots & \ddots & \vdots \\ \mathbb{V}_j^H Q_1 & \cdots & \mathbb{V}_j^H Q_{j-2} & H_{j,j-1} & H_{j,j} \end{bmatrix} \in \mathbb{C}^{n_j\times n_j}$ is no longer upper Hessenberg as soon as one inexact breakdown occurs, i.e., $\exists \ell,$ s.t., $Q_\ell \neq 0$.

Equation (12) can be rewritten in a more compact form as

$$A[U_k, \mathscr{V}_j] = \left[C_k, \mathscr{V}_j, [P_{j-1}, \widetilde{W}_j]\right] \underline{\mathscr{F}}_j,$$

so that the least-squares problem to be solved to compute the minimum residual norm solution associated with the generalized Arnoldi relation (12) becomes

$$Y_j = \underset{Y\in\mathbb{C}^{(k+n_j)\times p}}{\operatorname{argmin}} \left\|\Lambda_j - \underline{\mathscr{F}}_j Y\right\|_F, \tag{13}$$

with

$$\underline{\mathscr{F}}_j = \begin{bmatrix} I_k & & \mathcal{B}_j \\ & & \mathscr{L}_j \\ 0_{(n_j+p)\times k} & \mathbb{G}_{j-1} & E_j \\ & 0 & D_j \end{bmatrix} = \begin{bmatrix} \mathscr{F}_j \\ \mathbb{H}_j \end{bmatrix} \in \mathbb{C}^{(k+n_j+p)\times(k+n_j)} \tag{14}$$

and $\Lambda_j = \begin{bmatrix} 0_{k\times p} \\ \Lambda_1 \\ 0_{n_j\times p} \end{bmatrix} \in \mathbb{C}^{(k+n_j+p)\times p}$, where $\mathscr{F}_j = \begin{bmatrix} I_k & \mathcal{B}_j \\ 0_{n_j\times k} & \mathscr{L}_j \end{bmatrix} \in \mathbb{C}^{(k+n_j)\times(k+n_j)}$ and $\mathbb{H}_j = \begin{bmatrix} 0_{p\times k} & \mathbb{G}_{j-1} & E_j \\ & 0 & D_j \end{bmatrix} \in \mathbb{C}^{p\times(k+n_j)}$.

The numerical mechanism to select $\mathbb{V}_{j+1}$ out of $\left[P_{j-1}, \widetilde{W}_j\right]$ follows the same ideas as discussed in [1, 19] in the context of block GMRES. The governing idea consists in building an orthonormal basis for the directions that contribute the most to the individual residual norms and make them larger than a prescribed threshold τ. Specifically, the singular value decomposition (SVD) is applied to the least-square residual used in [1, 19] as

$$\Lambda_j - \underline{\mathscr{F}}_j Y_j = \mathbb{U}_{1,L}\Sigma_1\mathbb{U}_{1,R}^H + \mathbb{U}_{2,L}\Sigma_2\mathbb{U}_{2,R}^H, \tag{15}$$

where Σ_1 contains the p_{j+1} singular values larger than the prescribed threshold τ. Then we decompose $\mathbb{U}_{1,L} = \begin{pmatrix} \mathbb{U}_1^{(1)} \\ \mathbb{U}_1^{(2)} \end{pmatrix}$ in accordance with $\left[[C_k, \mathscr{V}_j], [P_{j-1}, \widetilde{W}_j]\right]$, that is $\mathbb{U}_1^{(1)} \in \mathbb{C}^{(k+n_j)\times p}$ and $\mathbb{U}_1^{(2)} \in$

$\mathbb{C}^{p\times p}$. Because, the objective is to construct orthonormal basis we consider $[\mathbb{W}_1, \mathbb{W}_2]$ unitary so that $\mathrm{Range}(\mathbb{W}_1) = \mathrm{Range}(\mathbb{U}_1^{(2)})$. The new set of orthonormal candidate vectors used to expand the search space

$$\mathbb{V}_{j+1} = \left[P_{j-1}, \widetilde{W}_j\right] \mathbb{W}_1 \tag{16}$$

is the one that contributes the most to the residual norms while

$$P_j = \left[P_{j-1}, \widetilde{W}_j\right] \mathbb{W}_2,$$

is the new set of orthogonal abandoned directions. Through this mechanism, directions that have been abandoned at a given iteration can be reintroduced, if the residual block has a large component along them. Furthermore, this selection strategy ensures that all the solutions have converged when p inexact breakdowns have been detected. We do not give the details of the calculation and refer to Section 3 of [19] for a complete description, but only state that via this decomposition the main terms that appear in Equation (12) can be computed incrementally.

2.4 Subspace recycling policies along with inexact breakdown

So far, we have not made any specific assumption on the definition of the recycling space U_k except that it has full column rank. In the context of subspace recycling, one key point is to specify what subspace is to be recycled at restart. At the cost of the extra storage of k vectors, block GCRO offers more flexibility than block GMRES in the choice of the recycling space. This extra storage, that enables us to remove the constraints to have the search space included in the residual space, allows us to consider any subspace to be deflated at restart. In particular any of the two classical alternatives, that are Rayleigh-Ritz procedure and harmonic-Ritz procedure, can be considered to compute targeted approximated eigenvectors to define U_k and C_k at restart.

Definition 1. *harmonic-Ritz projection.*
Consider a subspace $\mathcal{W}$ of $\mathbb{C}^n$. Given a general nonsingular matrix $A \in \mathbb{C}^{n\times n}$, $\lambda \in \mathbb{C}$ and $g \in \mathcal{W}$, (λ, g) is a harmonic-Ritz pair of A with respect to the space $\mathcal{W}$ if and only if

$$Ag - \lambda\, g \perp A\,\mathcal{W}$$

or equivalently,

$$\forall w \in \mathrm{Range}(A\,\mathcal{W}) \quad w^H\,(Ag - \lambda\, g) = 0.$$

The vector g is a harmonic-Ritz vector associated with the harmonic-Ritz value λ.

Definition 2. *Rayleigh-Ritz projection.*
Consider a subspace $\mathcal{W}$ of $\mathbb{C}^n$. Given a general nonsingular matrix $A \in \mathbb{C}^{n\times n}$, $\lambda \in \mathbb{C}$ and $g \in \mathcal{W}$, (λ, g) is a Rayleigh-Ritz pair of A with respect to the space $\mathcal{W}$ if and only if

$$Ag - \lambda\, g \perp \mathcal{W}$$

or equivalently,

$$\forall w \in \mathrm{Range}(\mathcal{W}) \quad w^H\,(Ag - \lambda\, g) = 0.$$

The vector g is a Rayleigh-Ritz vector associated with the Rayleigh Ritz value λ.

Once the maximum size of the search space has been reached, we have

$$A\widehat{\mathscr{W}}_m = \widehat{\mathscr{V}}_{m+1}\underline{\mathscr{F}}_m = \left[C_k, \mathscr{V}_m, [P_{m-1}, \widetilde{W}_m]\right]\underline{\mathscr{F}}_m, \tag{17}$$

$$X_m = X_1 + \widehat{\mathscr{W}}_m Y_m, \tag{18}$$

$$R_m = B - AX_m = \left[C_k, \mathscr{V}_m, [P_{m-1}, \widetilde{W}_m]\right](\Lambda_m - \underline{\mathscr{F}}_m Y_m), \tag{19}$$

$$Y_m = \underset{Y\in\mathbb{C}^{(k+n_m)\times p}}{\operatorname{argmin}} \|\Lambda_m - \underline{\mathscr{F}}_m Y\|_F, \quad \Lambda_m = [0_{p\times k}, \Lambda_1^T, 0_{p\times n_m}]^T. \tag{20}$$

Then, a restart procedure has to be implemented to possibly refine the spectral information to be recycled during the next cycle. Based on these equalities we will compute the approximated eigen-information as shown in Proposition 1 and then use it to define the new deflation basis U_k^{new} and its orthonormal image by A for C_k^{new} as described in Theorem 1.

Proposition 1. *At restart of IB-BGCRO-DR, the update of the recycling subspace for the next cycle relies on the computation of harmonic-Ritz vectors* $g_i^{(HR)} \in \operatorname{span}(\widehat{\mathscr{W}}_m)$*, or Rayleigh Ritz vectors* $g_i^{(RR)} \in \operatorname{span}(\widehat{\mathscr{W}}_m)$*, of* A *with respect to* $\widehat{\mathscr{W}}_m = [U_k, \mathscr{V}_m] \in \mathbb{C}^{n\times(k+n_m)}$.

- *The harmonic-Ritz pairs* $(\theta_i, \widehat{\mathscr{W}}_m g_i^{(HR)})$ *to be possibly used for the next restart satisfy*

$$\underline{\mathscr{F}}_m^H \underline{\mathscr{F}}_m g_i^{(HR)} = \theta_j \underline{\mathscr{F}}_m^H \widehat{\mathscr{V}}_{m+1}^H \widehat{\mathscr{W}}_m g_i^{(HR)}, \quad \text{for } 1 \le i \le n_m, \tag{21}$$

where $\widehat{\mathscr{V}}_{m+1}^H \widehat{\mathscr{W}}_m = \begin{bmatrix} C_k^H U_k & 0_{k\times n_m} \\ \mathscr{V}_m^H U_k & I_{n_m} \\ P_{m-1}^H U_k & \\ \widetilde{W}_m^H U_k & 0_{p\times n_m} \end{bmatrix} \in \mathbb{C}^{(k+n_m+p)\times(k+n_m)}$.

- *The Rayleigh Ritz pairs* $(\theta_i, \widehat{\mathscr{W}}_m g_i^{(RR)})$ *to be possibly used for the next restart satisfy*

$$\widehat{\mathscr{W}}_m^H \widehat{\mathscr{V}}_{m+1} \underline{\mathscr{F}}_m g_i^{(RR)} = \theta_j \widehat{\mathscr{W}}_m^H \widehat{\mathscr{W}}_m g_i^{(RR)}, \quad \text{for } 1 \le j \le n_m$$

where $\widehat{\mathscr{W}}_m^H \widehat{\mathscr{V}}_{m+1} = \begin{bmatrix} U_k^H C_k & U_k^H \mathscr{V}_m & U_k^H P_{m-1} & U_k^H \widetilde{W}_m \\ 0_{n_m\times k} & I_{n_m} & 0_{n_m\times p} & \end{bmatrix} \in \mathbb{C}^{(k+n_m)\times(k+n_m+p)}$ *and* $\widehat{\mathscr{W}}_m^H \widehat{\mathscr{W}}_m = \begin{bmatrix} U_k^H U_k & U_k^H \mathscr{V}_m \\ \mathscr{V}_m^H U_k & I_{n_m} \end{bmatrix} \in \mathbb{C}^{(k+n_m)\times(k+n_m)}$.

Proof. The proofs basically rely on some matrix computations as shortly described below:

- According to Definition 1, each harmonic-Ritz pair $(\theta_i, \widehat{\mathscr{W}}_m g_i^{(HR)})$ satisfies

$$\forall w \in \operatorname{Range}(A\widehat{\mathscr{W}}_m) \quad w^H (A\widehat{\mathscr{W}}_m g_i^{(HR)} - \theta_i \widehat{\mathscr{W}}_m g_i^{(HR)}) = 0,$$

which is equivalent to

$$(A\widehat{\mathscr{W}}_m)^H (A\widehat{\mathscr{W}}_m g_i^{(HR)} - \theta_i \widehat{\mathscr{W}}_m g_i^{(HR)}) = 0.$$

Substituting Equation (17) into the above one leads to

$$\left(\widehat{\mathscr{V}}_{m+1}\underline{\mathscr{F}}_m\right)^H \left(\widehat{\mathscr{V}}_{m+1}\underline{\mathscr{F}}_m g_i^{(HR)} - \theta_i \widehat{\mathscr{W}}_m g_i^{(HR)}\right) = 0. \tag{22}$$

Because $\widehat{\mathscr{V}}_{m+1} = [C_k, \mathscr{V}_m, [P_{m-1}, \widetilde{W}_m]]$ generated at the end of each cycle is orthonormal, Equation (22) becomes

$$\underline{\mathscr{F}}_m^H \underline{\mathscr{F}}_m g_i^{(HR)} - \theta_i \underline{\mathscr{F}}_m^H \widehat{\mathscr{V}}_{m+1}^H \widehat{\mathscr{W}}_m g_i^{(HR)} = 0,$$

which gives the formulation (21).

- Rayleigh Ritz pairs: using Definition 2 and similar arguments and matrix computation enable to derive the proof.

□

Depending on the region of the spectrum that is intended to be deflated (e.g., subspace associated with the smallest or/and largest eigenvalues in magnitude), a subset of k approximated eigenvectors is chosen among the n_m ones to define a space that will be used to span U_k^{new}. Then, we describe in Theorem 1 the update of U_k^{new} and its image C_k^{new} with respect to A at restart of IB-BGCRO-DR.

Theorem 1. *At restart of the IB-BGCRO-DR, if we intend to deflate the space* $\mathrm{span}([U_k, \mathcal{V}_m]G_k^{(*)})$ *where* $G_k^{(*)} = \left[g_1^{(*)}, ..., g_k^{(*)}\right]$ *with* $G_k^{(*)} = G_k^{(HR)}$ *or* $G_k^{(*)} = G_k^{(RR)}$ *is the set of vectors associated with the targeted eigenvalues, the matrices* U_k^{new} *and* C_k^{new} *to be used for the next cycle are defined by*

$$U_k^{new} = \widehat{\mathcal{W}_m} G_k^{(*)} R^{-1} = [U_k, \mathcal{V}_m] G_k^{(*)} R^{-1}, \tag{23}$$

$$C_k^{new} = \widehat{\mathcal{V}}_{m+1} Q = \left[C_k, \mathcal{V}_m, [P_{m-1}, \widetilde{W}_m]\right] Q, \tag{24}$$

where Q *and* R *are the factors of the reduced* QR*-factorization of the tall and skinny matrix* $\underline{\mathcal{F}}_m G_k^{(*)}$*, which* $AU_k^{new} = C_k^{new}$ *and* $(C_k^{new})^H C_k^{new} = I_k$.

Proof. Let Q and R be the factors of the reduced QR-factorization of the tall and skinny matrix $\underline{\mathcal{F}}_m G_k^{(*)}$. And right multiplying $G_k^{(*)}$ on both sides of Equation (17) leads to $A\widehat{\mathcal{W}_m} G_k^{(*)} = \widehat{\mathcal{V}}_{m+1} \underline{\mathcal{F}}_m G_k^{(*)} = \widehat{\mathcal{V}}_{m+1} QR$, that is equivalent to $A\widehat{\mathcal{W}_m} G_k^{(*)} R^{-1} = \widehat{\mathcal{V}}_{m+1} \underline{\mathcal{F}}_m G_k^{(*)} R^{-1} = \widehat{\mathcal{V}}_{m+1} Q$ concluding the proof as $\mathrm{span}(\widehat{\mathcal{W}_m} G_k^{(*)} R^{-1}) = \mathrm{span}(\widehat{\mathcal{W}_m} G_k^{(*)})$ and $\widehat{\mathcal{V}}_{m+1} Q$ is the product of two matrices with orthonormal columns so are its columns. □

Corollary 1. *The residual block at restart* $R_1^{new} = R_m^{old} = B - AX_1^{new}$ *with* $X_1^{new} = X_m^{old}$ *is orthogonal to* C_k^{new}.

Proof. $X_m^{old} = X_1 + \widehat{\mathcal{W}_m} Y_m$ where Y_m solves the least-squares problem (20) so that $(\Lambda_m - \underline{\mathcal{F}}_m Y_m) \in (\mathrm{Range}(\underline{\mathcal{F}}_m))^{\perp} = \mathrm{Null}(\underline{\mathcal{F}}_m^H)$. We also have $R_m^{old} = \widehat{\mathcal{V}}_{m+1} (\Lambda_m - \underline{\mathcal{F}}_m Y_m)$, consequently

$$\begin{aligned}
(C_k^{new})^H R_m^{old} &= \left(\widehat{\mathcal{V}}_{m+1} Q\right)^H \left(\widehat{\mathcal{V}}_{m+1} (\Lambda_m - \underline{\mathcal{F}}_m Y_m)\right) \\
&= \left(\widehat{\mathcal{V}}_{m+1} \underline{\mathcal{F}}_m G_k^{(*)} R^{-1}\right)^H \left(\widehat{\mathcal{V}}_{m+1} (\Lambda_m - \underline{\mathcal{F}}_m Y_m)\right) \\
&= R^{-H} G_k^{(*)\,H} \underbrace{\underline{\mathcal{F}}_m^H (\Lambda_m - \underline{\mathcal{F}}_m Y_m)}_{=0 \quad \text{because of (20)}} = 0.
\end{aligned}$$

□

2.5 A variant suited for flexible preconditioning

All what have been described in the previous sections are naturally extended to the right preconditioning case with a fixed preconditioner M, and the central equality writes as

$$A[U_k, M\mathcal{V}_m] = \left[C_k, \mathcal{V}_m, [P_{m-1}, \widetilde{W}_m]\right] \underline{\mathcal{F}}_m. \tag{25}$$

The least-squares problem to be solved to compute the minimum norm solution becomes

$$Y_m = \underset{Y \in \mathbb{C}^{(k+n_m)\times p}}{\operatorname{argmin}} \|\Lambda_m - \underline{\mathscr{F}}_m Y\|_F \,,$$

and the solution is

$$X_m = X_1 + [U_k, M\mathscr{V}_m]Y_m.$$

If we denote $\mathscr{M}_j$ a (possibly nonlinear) nonsingular preconditioning operator at iteration j and $\mathscr{M}_j(\mathbb{V}_j)$ denotes the action of $\mathscr{M}_j$ on a block vector $\mathbb{V}_j$, Equation (25) translates into

$$A[U_k, \mathscr{Z}_m] = \left[C_k, \mathscr{V}_m, [P_{m-1}, \widetilde{W}_m]\right] \underline{\mathscr{F}}_m \text{ with } \mathscr{Z}_m = [\mathscr{M}_1(\mathbb{V}_1), ..., \mathscr{M}_m(\mathbb{V}_m)]\,,$$

which writes in a more compact form as

$$A\widehat{\mathscr{Z}_m} = \widehat{\mathscr{V}}_{m+1}\underline{\mathscr{F}}_m \text{ with } \widehat{\mathscr{Z}_m} = [U_k, \mathscr{Z}_m] \text{ and } \widehat{\mathscr{V}}_{m+1} = \left[C_k, \mathscr{V}_m, [P_{m-1}, \widetilde{W}_m]\right]. \tag{26}$$

The solution update is $X_m = X_1 + [U_k, \mathscr{Z}_m]Y_m$. To keep the notation simple, we choose to keep the notation for quantities that have the same meaning as in the non-flexible case but of course will have different values.

In the context of flexible preconditioning many strategies for defining harmonic-Ritz vectors can be envisioned for GCRO-DR. Among those considered in [3], we follow the one with a lower computational cost required in solving the generalized eigenvalue problem, referred to as Strategy C in [3], thanks to the introducing of the third recycling subspace $\mathcal{W}_k$ that is initially empty but will be updated as in Equation (28). Furthermore, it also allows us to obtain very similar properties in the flexible preconditioning case to the ones we have exposed in the non-preconditioned case as shown in Section 2.4. We refer to Appendix A for another two strategies for approximating targeted eigen-information. Proposition 2 indicates that with an appropriate definition of the harmonic-Ritz vectors, all the properties of IB-BGCRO-DR extend to the flexible preconditioning variant denoted as IB-BFGCRO-DR.

Proposition 2. *At the end of a cycle of the IB-BFGCRO-DR algorithm, if the deflation space is built on the harmonic-Ritz vectors $g_i \in \operatorname{span}(\mathcal{W}_m)$ of $A\widehat{\mathscr{Z}_m}\mathcal{W}_m^\dagger$ with respect to $\mathcal{W}_m = [\mathcal{W}_k,\ \mathscr{V}_m] \in \mathbb{C}^{n\times(k+n_m)}$:*

1. *The harmonic-Ritz pairs $(\theta_i, \mathcal{W}_m g_i)$ for all restarts satisfy*

$$\underline{\mathscr{F}}_m^H \underline{\mathscr{F}}_m g_i = \theta_j \underline{\mathscr{F}}_m^H \widehat{\mathscr{V}}_{m+1}^H \mathcal{W}_m g_i, \quad \text{for } 1 \le i \le n_m, \tag{27}$$

where $\widehat{\mathscr{V}}_{m+1}^H \mathcal{W}_m = \begin{bmatrix} C_k^H\mathcal{W}_k & 0_{k\times n_m} \\ \mathscr{V}_m^H\mathcal{W}_k & I_{n_m} \\ P_{m-1}^H\mathcal{W}_k & 0_{p\times n_m} \\ \widetilde{W}_m^H\mathcal{W}_k & \end{bmatrix} \in \mathbb{C}^{(k+n_m+p)\times(k+n_m)}$,

2. *At restart, if $G_k = [g_1, \ldots, g_k]$ is associated with the k targeted eigenvalues, the matrices $\mathcal{W}_k^{new}$, U_k^{new} and C_k^{new} to be used for the next cycle are updated by*

$$\mathcal{W}_k^{new} = \mathcal{W}_m G_k R^{-1} = [\mathcal{W}_k, \mathscr{V}_m] G_k R^{-1}, \tag{28}$$

$$U_k^{new} = \widehat{\mathscr{Z}_m} G_k R^{-1} = [U_k, \mathscr{Z}_m] G_k R^{-1}, \tag{29}$$

$$C_k^{new} = \widehat{\mathscr{V}}_{m+1} Q = \left[C_k, \mathscr{V}_m, [P_{m-1}, \widetilde{W}_m]\right] Q,$$

where Q and R are the factors of the reduced QR-factorization of the tall and skinny matrix $\underline{\mathscr{F}}_m G_k$ ensuring $AU_k^{new} = C_k^{new}$ with $\left(C_k^{new}\right)^H C_k^{new} = I_k$.

3. *The residual at restart* $R_1^{new} = R_m^{old} = B - AX_1^{new}$ *with* $X_1^{new} = X_m^{old}$ *is orthogonal to* C_k^{new}.

Proof. The proof essentially follows the same arguments as the ones developed for IB-BGCRO-DR described in Section 2.4, and we refer the reader to the Appendix B for the details. □

We also mention that a closely related numerical technique that extends IB-BGMRES-DR in the flexible preconditioning context can be derived similarly although that is also novel. We refer to Appendix C where the resulting algorithm named IB-BFGMRES-DR is detailed and its properties are described.

3 Search space expansion policies governed by the stopping criterion

In this section we describe a few novel policies to expand the search space that generalize the original one considered for inexact breakdown detection [19]. In particular we first show how numerical criteria for detecting inexact breakdown can be consider for the search space expansion that can be tuned to ensure that a targeted threshold for a prescribed stopping criterion based on the individual backward error solution will eventually be satisfied. Secondly, we present how computational constraints can be taken into account, and combined with any of the previous numerical criteria, to best cope with the performance of the underlying computer architecture.

The inexact breakdown mechanism shortly described in Section 2.3 ensures that if all the singular values of the least squares residual are smaller than the threshold τ, then all the linear system residual norms are also smaller than τ (i.e., p inexact breakdowns have occurred). This is due to the following inequality

$$\forall i \quad \|b^{(i)} - Ax_j^{(i)}\| \leq \|B - AX_j\| = \|\Lambda_j - \underline{\mathscr{F}}_j Y_j\| = \sigma_{\max}(\Lambda_j - \underline{\mathscr{F}}_j Y_j) \leq \tau, \tag{30}$$

which follows from the fact that the 2-norm of a matrix is an upper-bound of the 2-norm of its individual columns and $\widehat{\mathscr{V}}_{j+1}$ has orthonormal columns.

3.1 Search space expansion policy governed by η_b

A classical stopping criterion for the solution of a linear system $Ax = b$ is based on backward error analysis and consists in stopping the iteration when

$$\eta_b(x_j) = \frac{\|b - Ax_j\|}{\|b\|} \leq \varepsilon. \tag{31}$$

This criterion was considered in [1] where it was consequently proposed to define $\tau = \varepsilon \min_{i=1,\ldots,p} \|b^{(i)}\|$. With this choice, when the iteration complies with Equation (30), we have

$$\eta_b(x_j^{(i)}) \leq \frac{\|b - Ax_j^{(i)}\|}{\min_{i=1,\ldots,p} \|b^{(i)}\|} \leq \varepsilon. \tag{32}$$

When the different right-hand sides have very different norms in magnitude, the subspace expansion associated with this criterion might not be effective as the upper-bound in Equation (32) will not be tight leading to enlarging the search space with directions that are not relevant (generating useless computation). In that context a better choice would be to better focus on the space expansion to reduce more the residual associated with right-hand side of large norm. For that purpose, the idea is to perform the SVD not directly on the least squares residual but on its scaled least squares residual.

Proposition 3. *Performing the SVD of the scaled least squares residual* $(\Lambda_j - \underline{\mathscr{F}}_j Y_j) D_{b,\varepsilon}$ *with threshold* $\tau = 1$ *and* $D_{b,\varepsilon} = \varepsilon^{-1} diag(\|b^{(1)}\|^{-1}, \cdots, \|b^{(p)}\|^{-1})$ *ensures that when* p *inexact breakdowns have occurred, so that the search space cannot be enlarged, the current individual iterates comply with the stopping criterion* (31).

Proof. This is a direct consequence of the following inequalities

$$\max_{i=1,..,p} \frac{\|b^{(i)} - Ax_j^{(i)}\|}{\varepsilon \|b^{(i)}\|} \leq \|(B - AX_j) D_{b,\varepsilon}\| = \|(\Lambda_j - \underline{\mathscr{F}}_j Y_j) D_{b,\varepsilon}\| \leq 1$$

that implies $\forall i \ \eta_b(x_j^{(i)}) \leq \varepsilon$. □

In some applications all the solutions associated with a block of right-hand sides do not need to be solved with the same accuracy. That is, we may have to solve a family of right-hand sides $B = [b^{(1)}, ..., b^{(p)}]$ with individual convergence thresholds $\varepsilon^{(i)}$ for the solution associated with each right-hand side $b^{(i)}$ $(i = 1, \cdots, p)$, thus we have a more general version of Equation (31) as

$$\eta_{b^{(i)}}(x_j^{(i)}) = \frac{\|b^{(i)} - Ax_j^{(i)}\|}{\|b^{(i)}\|} \leq \varepsilon^{(i)}. \tag{33}$$

In that context, the subspace expansion policy can be easily adapted to ensure the convergence for each individual accuracy.

Corollary 2. *Performing the SVD of the scaled least squares residual* $(\Lambda_j - \underline{\mathscr{F}}_j Y_j) D_{b,\varepsilon_i}$ *with threshold* $\tau = 1$ *and* $D_{b,\varepsilon_i} = diag((\varepsilon_1 \|b^{(1)}\|)^{-1}, \cdots, (\varepsilon_p \|b^{(p)}\|)^{-1})$ *ensures that when* p *inexact breakdowns have occurred the current individual iterates comply with the stopping criterion* (33).

3.2 Search space expansion policy governed by $\eta_{A,b}$

One can also adapt the expansion policy described in the previous section to the situation where the stopping criterion is based on the normwise backward error on A and b, defined by

$$\eta_{A,b}(x_j) = \frac{\|b - Ax_j\|}{\|b\| + \|A\| \ \|x_j\|} \leq \varepsilon. \tag{34}$$

It suffices to define accordingly the scaled least squares residual in the SVD that is involved in the search space expansion. We notice that this type of stopping criterion will have a computational penalty as the approximations of all individual iterations have to be computed.

Corollary 3. *Performing the SVD of the scaled least squares residual* $(\Lambda_j - \underline{\mathscr{F}}_j Y_j) D_{A,b,\varepsilon}$ *with threshold* $\tau = 1$ *and* $D_{A,b,\varepsilon} = \varepsilon^{-1} diag((\|A\|\|x_j^{(1)}\| + \|b^{(1)}\|)^{-1}, \cdots, (\|A\|\|x_j^{(p)}\| + \|b^{(p)}\|)^{-1})$ *ensures that when* p *inexact breakdowns have occurred, the current individual iterates comply with the stopping criterion* (34).

We do not develop further these ideas but similarly we could define expansion policies where for each solution we can select either η_b or $\eta_{A,b}$ as stopping criterion with individual threshold setting.

The occurrence of p inexact breakdowns is a sufficient condition that ensures the convergence of the p solution vectors, but the convergence might happen before and a more classic stopping criterion can be accommodated at a low computational cost. Given the norms of true residuals are very close to those of the least squares residuals when the loss of orthogonality of the generated block Krylov basis is not too

serious, one can also check the convergence by looking at the norm of the least squares residual, which is easy to compute. Let $Q_j^{LS} R_j^{LS}$ be a full QR-factorization of $\underline{\mathscr{F}}_j$ (i.e., Q_j^{LS} is unitary) , then

$$\Lambda_j - \underline{\mathscr{F}}_j Y_j = Q_j^{LS} \begin{pmatrix} 0_{(n_j+k)\times p} \\ R_j^{\ell s} \end{pmatrix}, \tag{35}$$

where $R_j^{\ell s} \in \mathbb{C}^{p\times p}$ are the last p rows of $(Q_j^{LS})^H \Lambda_j$ so that $\|b^{(i)} - Ax_j^{(i)}\| = \|R_j^{\ell s}(:,i)\|$. Those residual norm calculations are part of the stopping criterion based on η_b or $\eta_{A,b}$

3.3 Search space expansion policy governed by computational performance

Based on any of these expansion policies, the abandoned directions at a given iteration might be reintroduced in a subsequent one, thereby we can trade on the considered numerical policy and select for the subspace expansion only a subset of those eligible. In particular, it might be relevant to choose a prescribed block size p^{CB} (here the superscript ^{CB} stands for Computational Blocking) that is suited to best cope with the computational features on a given platform rather than selecting the numerical block size p_{j+1} defined as the number of singular values larger than the prescribed threshold $\tau = 1$. In that respect, we consider a subspace expansion policy so that the block size at the end of step j is defined as $p_{j+1}^{CB} = \min(p^{CB}, p_{j+1})$. We refer this variant as Inexact Breakdown Block GCRO-DR with computational blocking (denoted by IB-BGCRO-DR-CB).

Note that all the subspace expansion policies discussed in Section 3 could be applied to any other block minimum residual norm methods equipped with the inexact breakdown mechanism such as the IB-BGMRES [19] and IB-BGMRES-DR [1] algorithms.

4 Remarks on some computational and algorithmic aspects

The mathematical description made in the previous section assumes exact calculation. In practice, the numerical behavior of the algorithm does depend on numerical algorithm selected to perform the computation. In particular, all the above descriptions assume the orthonormality of the residual basis that ensures the norm equality of the true linear system residual and their least squares counterpart which governs the numerical search space expansion policies described in the previous section. In our numerical experiments, we use the Modified Gram-Schmidt (MGS) algorithm whenever orthogonality is prescribed. For the sake of consistency, MGS is used for performing the reduced QR-factorization as well as the Arnoldi steps that rely on the MGS-Ruhe algorithm [20] so that the orthogonalization of the residual basis is performed one vector at a time (and not as described in Algorithm 1 that was used to introduce the notations). For the sake of conciseness, we do not necessarily give the full technical details of what we briefly expose in the core of the paper but sometimes refer to a particular part in the appendix.

4.1 Inexact breakdown and re-orthogonalization at restart

For the sake of simplicity of exposure, in the previous sections we made the assumption that the initial residual block was of full rank. In practice, this constraint can be removed by applying the inexact breakdown (IB) mechanism to the initial residual block. In that case, only a subspace of the space spanned by the columns of the initial residual block will be selected to define the first search space and the abandoned directions are kept in the basis of the residual space. This has two main consequences:

1. The first iteration needs some extra attentions to set up the initial basis $\mathbb{V}_1$ and abandoned directions P_0 defined in Equation (11).

2. A consequence of having abandoned directions in the first search space is that the projection of the initial residual block in the residual space, that defines the right-hand side of the least squares residual solved at each block iteration, will no longer have the nested block structure that is expanded by a $p \times p$ zero block at each block iteration as presented in Equation (20).

Without loss of generality, let us present the inexact breakdown and re-orthogonalization at restart where the recycling subspace U_k^{new} and C_k^{new} are defined by Equation (23) and (24), so that mathematically $AU_k^{new} = C_k^{new}$ and $(C_k^{new})^H C_k^{new} = I_k$ and the initial residual block $R_1^{new} = R_1$ in Corollary 1 is orthogonal to C_k^{new}. For a prescribed stopping criterion and convergence threshold, let us denote D_ε the diagonal matrix used to select the space expansion described in the Section 3. Let

$$R_1 D_\varepsilon = [\mathbb{V}_1^{new}, P_0^{new}] \begin{bmatrix} \Sigma_{p_1} & \\ & \Sigma_{q_1} \end{bmatrix} \mathbb{V}_{R_1}^H = [\mathbb{V}_1^{new}, P_0^{new}] \hat{\Lambda}_1', \tag{36}$$

where $\mathbb{V}_1^{new} \in \mathbb{C}^{n \times p_1}$, $P_0^{new} \in \mathbb{C}^{n \times q_1}$ with $p_1 + q_1 = p$, and Σ_{p_1} contains the p_1 singular values of $R_1 D_\varepsilon$ larger than or equal to the prescribed τ, and Σ_{q_1} the ones smaller than τ.

We first perform a MGS re-orthogonalization of the columns of $[C_k^{new}, [\mathbb{V}_1^{new}, P_0^{new}]]$ that writes

$$[C_k^{new}, [\mathbb{V}_1^{new}, P_0^{new}]] = [C_k, [\mathbb{V}_1, P_0]] \begin{bmatrix} R_{11} & R_{12} \\ & R_{22} \end{bmatrix}, \tag{37}$$

where all the columns of $[C_k, [\mathbb{V}_1, P_0]]$ are orthogonal to each other, $\begin{bmatrix} R_{11} & R_{12} \\ & R_{22} \end{bmatrix} \in \mathbb{C}^{(k+p)\times(k+p)}$ is an upper triangular matrix with $R_{11} \in \mathbb{C}^{k\times k}$ and $R_{22} \in \mathbb{C}^{p\times p}$. Next, we update $U_k = U_k^{new} R_{11}^{-1}$ to satisfy Equation (3), and $\mathscr{V}_1 = \mathbb{V}_1$ will serve to span the first search space and P_0 will be abandoned for this first block iteration that will be run as follows.

1. Form $W_1 = A\mathbb{V}_1$ and orthogonalize (using MGS) it against the set of orthonormal vectors that are part of the residual space $[C_k, \mathbb{V}_1, P_0]$ which enables the computation of the entries of $\mathcal{B}_1 = C_k^H W_1$, $\mathscr{L}_{1,1} = \mathbb{V}_1^H W_1$ and $E_1 = P_0^H W_1$.

2. The resulting block $\bar{W}_1$ formally writes $\bar{W}_1 = W_1 - C_k\mathcal{B}_1 - \mathbb{V}_1\mathscr{L}_{1,1} - P_0 E_1$ with $\bar{W}_1 = \widetilde{W}_1 D_1$ its reduced QR-factorization.

3. In matrix form the above relations also writes

$$W_1 = A\mathbb{V}_1 = \left[C_k, \mathbb{V}_1, [P_0, \widetilde{W}_1]\right] \begin{bmatrix} \mathcal{B}_1 \\ \mathscr{L}_{1,1} \\ E_1 \\ D_1 \end{bmatrix}.$$

So that we have the first Arnoldi-like relation

$$A[U_k, \mathbb{V}_1] = \left[C_k, \mathbb{V}_1, [P_0, \widetilde{W}_1]\right] \underline{\mathscr{F}}_1 \tag{38}$$

with

$$\underline{\mathscr{F}}_1 = \begin{bmatrix} I_k & \mathcal{B}_1 \\ 0_{(p_1+p)\times k} & \mathscr{L}_{1,1} \\ & \widetilde{\mathbb{H}}_1 \end{bmatrix} \in \mathbb{C}^{(k+p_1+p)\times(k+p_1)} \text{ and } \widetilde{\mathbb{H}}_1 = \begin{bmatrix} E_1 \\ D_1 \end{bmatrix} \in \mathbb{C}^{p\times p_1}.$$

4. Next, define the minimum norm solution $X_2 = X_1 + [U_k, \mathbb{V}_1]Y$ and notice that R_1 belongs to the space $[C_k, \mathbb{V}_1, P_0, \widetilde{W}_1]$ where its components in this orthogonal basis are given by $[C_k, \mathbb{V}_1, P_0, \widetilde{W}_1]^H R_1$. From Equation (38) we have

$$\begin{aligned} \|B - AX_2\|_F &= \|R_1 - A\,[U_k, \mathbb{V}_1]\,Y\|_F = \|R_1 - [C_k, \mathbb{V}_1, P_0, \widetilde{W}_1]\underline{\mathscr{F}}_1 Y\|_F \\ &= \|[C_k, \mathbb{V}_1, P_0, \widetilde{W}_1]^H R_1 - \underline{\mathscr{F}}_1 Y\|_F \\ &= \|[C_k, \mathbb{V}_1, P_0, \widetilde{W}_1]^H [\mathbb{V}_1^{new}, P_0^{new}]\hat{\Lambda}_1 - \underline{\mathscr{F}}_1 Y\|_F, \end{aligned}$$

because from Equation (36), we have

$$R_1 = [\mathbb{V}_1^{new}, P_0^{new}]\hat{\Lambda}_1' D_\varepsilon^{-1} = [\mathbb{V}_1^{new}, P_0^{new}]\hat{\Lambda}_1 \text{ with } \hat{\Lambda}_1 = \hat{\Lambda}_1' D_\varepsilon^{-1}. \tag{39}$$

So that from (37), the right-hand side of the above least squares residual reads

$$\begin{aligned} \Lambda_1 &= [C_k, \mathbb{V}_1, P_0, \widetilde{W}_1]^H [\mathbb{V}_1^{new}, P_0^{new}]\hat{\Lambda}_1 = [C_k, \mathbb{V}_1, P_0, \widetilde{W}_1]^H [C_k R_{12} + [\mathbb{V}_1, P_0]R_{22}]\hat{\Lambda}_1 \\ &= \left([C_k, \mathbb{V}_1, P_0, \widetilde{W}_1]^H C_k R_{12} + [C_k, \mathbb{V}_1, P_0, \widetilde{W}_1]^H [\mathbb{V}_1, P_0]R_{22}\right)\hat{\Lambda}_1 \\ &= \begin{bmatrix} R_{12} \\ 0_{(p_1+p)\times p} \end{bmatrix}\hat{\Lambda}_1 + \begin{bmatrix} 0_{k\times p_1} & 0_{k\times q_1} \\ I_{p_1} & 0_{p_1\times q_1} \\ 0_{q_1\times p_1} & I_{q_1} \\ 0_{p_1\times p_1} & 0_{p_1\times q_1} \end{bmatrix} R_{22}\hat{\Lambda}_1 \in \mathbb{C}^{(k+p_1+p)\times p}. \end{aligned} \tag{40}$$

5. Compute Y_1 the solution of the first new least-squares problem

$$Y_1 = \underset{Y\in\mathbb{C}^{(k+p_1)\times p}}{\operatorname{argmin}} \|\Lambda_1 - \underline{\mathscr{F}}_1 Y\|_F\,.$$

6. Execute the search space expansion policy following the IB principles

   (a) compute the SVD of the scaled least squares residual

   $$(\Lambda_1 - \underline{\mathscr{F}}_1 Y_1)\,D_\varepsilon = \mathbb{U}_{1,L}\Sigma_1\mathbb{V}_{1,R}^H + \mathbb{U}_{2,L}\Sigma_2\mathbb{V}_{2,R}^H, \text{ where } \sigma_{\min}(\Sigma_1) \geq 1 > \sigma_{\max}(\Sigma_2).$$

   (b) Compute $\mathbb{W}_1$ and $\mathbb{W}_2$ such that $\mathrm{Range}(\mathbb{W}_1) = \mathrm{Range}(\mathbb{U}_1^{(2)}) \in \mathbb{C}^{p\times p_2}$ with $\mathbb{U}_{1,L} = \begin{pmatrix} \mathbb{U}_1^{(1)} \\ \mathbb{U}_1^{(2)} \end{pmatrix} \in \mathbb{C}^{(k+p_1+p)\times p_2}$, $[\mathbb{W}_1, \quad \mathbb{W}_2]$ is unitary and $\mathbb{W}_2 \in \mathbb{C}^{p\times q_2}$ with $p_2 + q_2 = p$.

   (c) Compute the new orthonormal matrices $\mathbb{V}_2$ and P_1 as

   $$\mathbb{V}_2 = [P_0, \widetilde{W}_1]\mathbb{W}_1 \in \mathbb{C}^{n\times p_2},\ P_1 = [P_0, \widetilde{W}_1]\mathbb{W}_2 \in \mathbb{C}^{n\times q_2},$$

   as well as the last block row matrix $\mathscr{L}_{2,:}$ of $\underline{\mathscr{L}}_1$ and $\mathbb{G}_1$ as

   $$\mathscr{L}_{2,:} = \mathbb{W}_1^H\widetilde{\mathbb{H}}_1 \in \mathbb{C}^{p_2\times p_1},\ \mathbb{G}_1 = \mathbb{W}_2^H\widetilde{\mathbb{H}}_1 \in \mathbb{C}^{q_2\times p_1}.$$

7. Set $\underline{\mathscr{L}}_1 = \begin{pmatrix} \mathscr{L}_1 \\ \mathscr{L}_{2,:} \end{pmatrix} \in \mathbb{C}^{(p_1+p_2)\times p_1} = \mathbb{C}^{n_2\times p_1}$.

Whenever an inexact breakdown is detected in R_1, some of its components (along P_0^{new}) are firstly abandoned but could be reintroduced in some subsequent iterations. One of the consequences, is that the last q_1 columns of the least squares right-hand side problem will evolve from one iteration to the next, depending on how some of the P_0^{new} directions will be re-introduced in the search space along the iterations. There is a way to incrementally update the least squares right-hand side to be discussed in the next proposition.

Proposition 4. *At each iteration of IB-BGCRO-DR, the new least-squares problem reads*

$$Y_{j+1} = \underset{Y \in \mathbb{C}^{(k+n_{j+1})\times p}}{\operatorname{argmin}} \left\| \Lambda_{j+1} - \underline{\mathscr{F}}_{j+1} Y \right\|_F, \quad \Lambda_{j+1} \in \mathbb{C}^{(k+n_{j+1}+p)\times p}, \quad j = 0, 1, 2, \cdots \tag{41}$$

with the updated right-hand sides being

$$\Lambda_{j+1} = \begin{bmatrix} R_{12} \\ 0_{(n_j+p+p_{j+1})\times p} \end{bmatrix} \hat{\Lambda}_1 + \begin{bmatrix} 0_{k\times p_1} & 0_{k\times q_1} \\ \begin{bmatrix} I_{p_1} \\ 0_{(n_j+p-p_1)\times p_1} \end{bmatrix} & \Phi_{j+1} \\ 0_{p_{j+1}\times p_1} & 0_{p_{j+1}\times q_1} \end{bmatrix} R_{22}\, \hat{\Lambda}_1, \tag{42}$$

where $\Phi_{j+1} = \begin{bmatrix} \Phi_j(1:n_j,:) \\ [\mathbb{W}_1, \mathbb{W}_2]^H \begin{bmatrix} \Phi_j(n_j+1:n_j+q_j,:) \\ 0_{p_j\times q_1} \end{bmatrix} \end{bmatrix} \in \mathbb{C}^{(n_j+p)\times q_1}$ *for* $j = 0, 1, 2, \cdots$, *with* $\Phi_1 = \begin{bmatrix} 0_{p_1\times q_1} \\ I_{q_1} \end{bmatrix} \in \mathbb{C}^{p\times q_1}$, $q_j = p - p_j (j > 0)$ *and* $[\mathbb{W}_1, \mathbb{W}_2]$ *is unitary as defined in the search space expansion algorithm based on IB principles,* $R_{12} \in \mathbb{C}^{k\times p}$ *and* $R_{22} \in \mathbb{C}^{p\times p}$ *are two block components of the upper triangular matrix as shown in the right-hand side of Equation* (37).

Proof. Refer to Appendix D the proving details. □

Based on the above discussions, the IB-BGCRO-DR algorithm with inexact breakdown detection in the initial residual block and updated right-hand side of the least squares residual is presented in Algorithm 2 for solving a series of linear systems with slowly-changing left-hand sides.

4.2 Solution of the least-squares problem and cheap SVD calculation of the scaled least squares residual

Computing the full QR-factorization of the matrices involved in the least-squares problems allows us to reuse its Q factor to compte the SVD of the least squares residual using a QR-SVD algorithm such that the the actual SVD decomposition is performed on a $p \times p$ block $R_j^{\ell s} D_\varepsilon$, where $R_j^{\ell s}$ appeared in the right-hand side of Equation (35), at each iteration (we refer to Appendix E for the details of this calculation). Note that this observation applies naturally to the IB-BGMRES [19] and IB-BGMRES-DR [1] algorithms as well.

5 Numerical experiments

In the following sections we illustrate the different numerical features of the novel algorithm introduced above. For the sake of comparison, in some of the experiments we also display results of closely related block methods such as BGCRO-DR [16, 17, 22, 29] or IB-BGMRES-DR [1]. All the numerical experiments have been run using a MATLAB prototype, so that the respective performances of the algorithms are evaluated in term of number of matrix-vector products, denoted as $mvps$ (and preconditioner applications in the preconditioned case) required to converge.

For each set of block of right-hand sides, referred to as a family, the block initial guess is equal to $0 \in \mathbb{C}^{n\times p}$, where p is the number of right-hand sides. The block right-hand side $B = [b^{(1)}, b^{(2)}, \ldots, b^{(p)}] \in \mathbb{C}^{n\times p}$ is composed of p linearly independent vectors generated randomly (using the same seed when block methods are compared). While any part of the spectrum could be considered to define the recycling space we consider for all the experiments the approximated eigenvectors associated with the k smallest approximated eigenvalues in magnitude. The maximum dimension of the search space in each cycle is

Algorithm 2 IB-BGCRO-DR for slowly-changing left-hand sides and massive number of right-hand sides

Require: $A \in \mathbb{C}^{n\times n}$ left-hand side of current family (supposed not vary much compared to previous one)
Require: $B \in \mathbb{C}^{n\times p}$ the block of right-hand-sides and $X_0 \in \mathbb{C}^{n\times p}$ the block initial guess
Require: m maximum number of Arnoldi step within a cycle
Require: p^{CB} a given constant number satisfying $1 \leq p^{CB} \leq p$ for computational blocking
Require: $D_\varepsilon \in \mathbb{C}^{p\times p}$ a diagonal matrix used to select the space expansion described in the Section 3
Require: $U_k, C_k \in \mathbb{C}^{n\times k}$ the recycling subspaces supposed be empty for the first family and obtained after solving previous slow-changing family
Compute $R_0 = B - AX_0$
/ Some families have already been solved ? */*
if the recycling space is not empty, $U_k \neq 0$ **then**
  Apply the reduced QR-factorization to AU_k for updating U_k and C_k for the current family such that the U_k and C_k satisfy Equation (3) and (4). Compute R_1 and X_1 as described in Equation (6)
else
  Set $R_1 = R_0$, $X_1 = X_0$, $U_k = 0$, $C_k = 0$
end if
/ Loop over the restarts */*
while the stopping criterion based on Section 3.1 or 3.2 is not met **do**
  Apply inexact breakdown detection in the scaled (least squares) residual block following Section 4.1
  / Arnoldi loop */*
  for $j = 2, 3, \ldots, m$ **do**
    Orthogonalize $A\mathbb{V}_j$ against C_k as $W_j = (I - C_kC_k^H)A\mathbb{V}_j$. Then orthogonalize W_j against previous block orthonormal vector $\mathscr{V}_j = [\mathbb{V}_1, \ldots, \mathbb{V}_j]$ as

$$W_j = A\mathbb{V}_j - C_kC_k^HA\mathbb{V}_j - \mathscr{V}_j\mathscr{L}_{1,1:j}, \text{ where } \mathscr{L}_{1,1:j} = \mathscr{V}_j^H(W_j) = \mathscr{V}_j^H(A\mathbb{V}_j) \text{ is a block column matrix}$$

    Set $\mathscr{L}_j = \begin{bmatrix}\underline{\mathscr{L}}_{j-1}, & \mathscr{L}_{1,1:j}\end{bmatrix} \in \mathbb{C}^{n_j\times n_j}$, $\mathcal{B}_j = \begin{bmatrix}\mathcal{B}_{j-1}, & C_k^HA\mathbb{V}_j\end{bmatrix} \in \mathbb{C}^{k\times n_j}$
    Orthogonalize W_j against P_{j-1} and carry out its reduced QR-factorization as

$$\widetilde{W}_jD_j = W_j - P_{j-1}E_j, \text{ where } E_j = P_{j-1}^HW_j$$

    Compute Y_j by solving the least squares residual described in Equation (13) (or (41)) with $\underline{\mathscr{F}}_j$ shown in Equation (14) composed by $\mathscr{F}_j$ and $\mathbb{H}_j$ but with the updated right-hand side Λ_j as shown in Equation (42) instead
    if the stopping criterion is met **then**
      return $X_j = X_1 + [U_k, \mathscr{V}_j]Y_j$, U_k and C_k
    end if
    Singular value decomposition of the residuals scaled by D_ε

$$(\Lambda_j - \underline{\mathscr{F}}_jY)D_\varepsilon = \mathbb{U}_{1,L}\Sigma_1\mathbb{V}_{1,R}^H + \mathbb{U}_{2,l}\Sigma_2\mathbb{V}_{2,R}^H \text{ with } \sigma_{\min}(\Sigma_1) \geq 1 > \sigma_{\max}(\Sigma_2)$$

    if Computational blocking of Section 3.3 is activated **then**
      $\mathbb{U}_{1,L} = \mathbb{U}_{1,L}(:, 1 : p_j^{CB})$ with $p_j^{CB} = min(p^{CB}, nl_{\Sigma_1})$, nl_{Σ_1} refers to column number of Σ_1
    end if
    Following item 6 described in Section 4.1 for computing $\mathbb{W}_1$ and $\mathbb{W}_2$
    Compute orthonormal matrices $\mathbb{V}_{j+1}$ and P_j, the last block row matrix $\mathscr{L}_{j+1,:}$ of $\underline{\mathscr{L}}_j$, and G_j as

$$\mathbb{V}_{j+1} = \left[P_{j-1}, \widetilde{W}_j\right]\mathbb{W}_1, P_j = \left[P_{j-1}, \widetilde{W}_j\right]\mathbb{W}_2, \mathscr{L}_{j+1,:} = \mathbb{W}_1^H\mathbb{H}_j, \mathbb{G}_j = \mathbb{W}_2^H\mathbb{H}_j, \underline{\mathscr{L}}_j = \begin{pmatrix}\mathscr{L}_j \\ \mathscr{L}_{j+1,:}\end{pmatrix}$$

  end for
  / Restart procedure */*
  Compute the solution X_m as described in Equation (18) and residual R_m according to (19)
  Compute the targeted harmonic-Ritz vectors $G_k = [g_1, ..., g_k]$ by solving the generalized eigenvalue problem (21) described in Proposition 1
  Update the values of U_k and C_k respectively by Equation (23) and (24) described in Theorem 1
  Restart with $X_1 = X_m$, $\widehat{\mathscr{V}}_{m+1}$, $R_1^{LS} = \Lambda_m - \underline{\mathscr{F}}_mY_m$ ($R_1 = R_m = \widehat{\mathscr{V}}_{m+1}R_1^{LS}$)
end while
return X_j for approximation of the current family; U_k, C_k for the next family to be solved

set to be $m_d = 15 \times p$. To illustrate the potential benefit of IB-BGCRO-DR when compared to another block solver, we consider the overall potential gain when solving a sequence of ℓ families defined as

$$\text{Gain } (\ell) = \frac{\sum_{s=1}^{\ell} \#mvps \text{ (method)}^{(s)}}{\sum_{s=1}^{\ell} \#mvps \text{ (IB-BGCRO-DR)}^{(s)}}. \tag{43}$$

5.1 Rayleigh Ritz versus harmonic-Ritz approach exploited for recycling subspace

To illustrate the flexibility of subspace recycling in IB-BGCRO-DR as discussed in Section 2.4, both the harmonic-Ritz (HR) and Rayleigh-Ritz (RR) projections are considered to construct the recycled subspace; the associated algorithms are referred to as IB-BGCRO-DR(HR) and IB-BGCRO-DR(RR). Following the spirit of the test examples considered in [11] we consider bidiagonal matrices of size 5000 with upper diagonal unity so that their spectrum is defined by their diagonal entries; we denote them Matrix 1 and Matrix 2. Matrix 1 has diagonal entries $0.1, 1, 2, 3, \ldots, 4999$ and Matrix 2 has diagonal entries $10.1, 10.2, \ldots, 20, 21, \ldots, 4920$. We consider experiments with a family size $p = 20$, the size of the recycled space $k = 30$ and the maximal dimension of the search space $m_d = 300$. In Figure 1 we display some experimental results. The graphs on the left give the envelope of the convergence histories of the p backward errors as a function of the number of matrix-vector products ($mvps$) for the first three families. On the right graphs we depict $mvps$ for each of the 30 families. For Matrix 1, one can observe that the HR-projection does capture a space that slows down the initial convergence once the first family has been solved; that is, for families 2 and 3 the converge histories do not exhibit anymore any plateau. On that example the RR-projection does not capture a recycled space that helps much the convergence as the three convergence histories exhibit very similar pattern. For Matrix 2, both RR and HR projections work pretty much the same. In Table 1, we report the total required $mvps$ for the two matrix examples for 3 and 30 families. Those results do not attempt to highlight that one projection is superior to the other one, but simply illustrate the flexibility of the GCRO approach to accommodate both. The selection or discussion of the best suited projection method is out of the scope of this paper.

Number of families	Matrix	Method	$mvps$
3	Matrix 1	IB-BGCRO-DR(HR)	**7182**
		IB-BGCRO-DR(RR)	7583
30	Matrix 1	IB-BGCRO-DR(HR)	**68262**
		IB-BGCRO-DR(RR)	71690
3	Matrix 2	IB-BGCRO-DR(HR)	13981
		IB-BGCRO-DR(RR)	**13430**
30	Matrix 2	IB-BGCRO-DR(HR)	138247
		IB-BGCRO-DR(RR)	**137453**

Table 1: Numerical results of IB-BGCRO-DR with recycling subspace generated by RR or HR-projection for Matrix 1 and Matrix 2 with $p = 20$, $m_d = 300$ and $k = 30$.

In the rest of this paper, only the HR projection is considered to build recycling subspace used in the GCRO-DR like methods. Besides, the bidiagonal Matrix 1 is chosen as the constant left-hand sides in following Section 5.2- 5.6, in which the related parameters are likewise set to be $p = 20$, $k = 30$ and $m_d = 300$ defaultly.

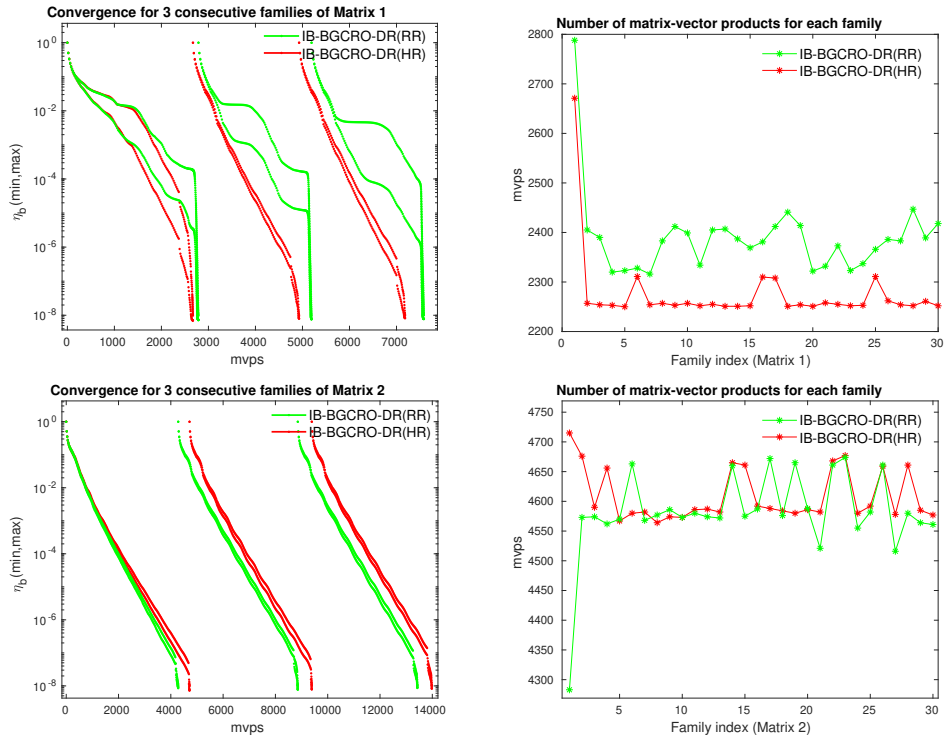

Figure 1: History of bidiagonal Matrix 1 and Matrix 2 ($p = 20$, $m_d = 300$ and $k = 30$). Left: convergence histories of the largest/smallest backward errors $\eta_{b^{(i)}}$ at each $mvps$ for 3 consecutive families. Right: consumed number of $mvps$ versus family index.

5.2 Comparing IB-variants with two different inexact breakdown thresholds τ

According to Equation (32) appeared in previous Section 3.1, the inexact breakdown (IB)-threshold we adopted in this work satisfy $\tau = 1$. Specifically, assume all the solutions corresponding to each single right-hand sides $\eta_b(x_j^{(i)})$ as described in left-hand side of Equation (32) converge to the same convergence threshold ε, when p inexact breakdowns have occurred, we have,

$$\frac{||b^{(i)} - Ax_j^{(i)}||}{||b^{(i)}|| \times \varepsilon} \leq \frac{||B - AX_j||}{||b^{(i)}|| \times \varepsilon} \leq \left\| \left(\Lambda_1 - \underline{\mathscr{F}}_j Y_j\right) D_\varepsilon \right\| \leq \tau \text{ for } \forall i \in \{1, \cdots, p\}, \tag{44}$$

where $D_\varepsilon = \varepsilon^{-1}\,\mathrm{diag}\,(||b^{(1)}||^{-1}, \cdots, ||b^{(p)}||^{-1}) \in \mathbb{C}^{p\times p}$ with $\tau = 1$. Comparing $\tau = 1$ appeared in the right-hand side of Equation (44) with the original version of IB-threshold $\tau = \varepsilon \min\limits_{i=1,\ldots,p} ||b^{(i)}||$ described in Equation (3.17) of [1, Section 3.3] (which is specially denoted as min-IB-threshold in here for distinguishing it from $\tau = 1$), we conclude that the IB-variants (like IB-BGCRO-DR or IB-BGMRES-DR) with the IB-threshold $\tau = 1$ show clear benefit especially when the norm of each single right-hand side $||b^{(i)}||$ is very different in magnitude, which may give rise to the $\min\limits_{i=1,\ldots,p} ||b^{(i)}||$ be quite different from some others that with larger norms thus further leads to the min-IB-threshold fails to detect IB of these columns effectively. This is illustrated by the results shown in Figure 2, in which the min-IB-BGCRO-DR refers to the IB-BGCRO-DR algorithm with the min-IB-threshold with the form as $\tau = \varepsilon \min\limits_{i=1,\ldots,p} ||b^{(i)}||$ while IB-BGCRO-DR is the one with the IB-threshold $\tau = 1$ proposed and adopted in this paper.

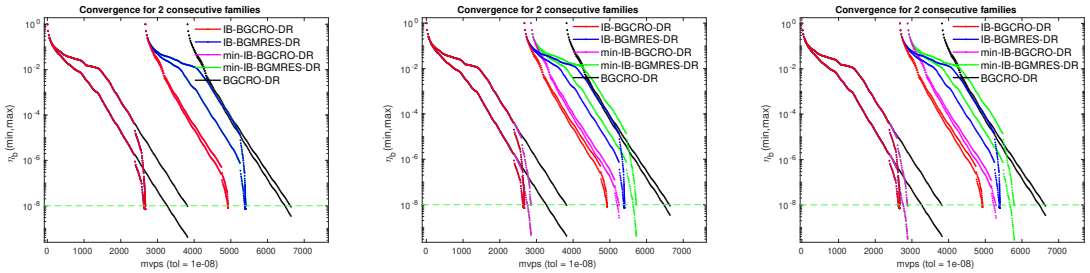

Figure 2: Convergence histories of the largest/smallest backward errors $\eta_{b^{(i)}}$ at each $mvps$ for Section 5.2 with different scaling size of the columns of the RHSs. Comparison the two IB-variants with two different form of IB-threshold by solving Matrix 1 ($p = 20$, $m_d = 300$, $\varepsilon = 10^{-8}$ and $k = 30$). Left: $B = rand(n, p)$. Middle: $B = rand(n, p)$ and then multiply 20 to the first $\frac{p}{2}$ columns of B. Right: be the same as the Middle case except for multiplying 50 instead.

5.3 Benefits of recycling between the families

To illustrate the benefits of recycling spectral information from one family to next as well as the computational saving due to the inexact breakdown (IB) mechanism, we first report on experiments with BGCRO-DR, IB-BGCRO-DR and IB-BGMRES-DR on a series of linear systems with constant left-hand side. We consider experiments with a family size $p = 20$, the size of the recycled space $k = 30$ and the maximal dimension of the search space $m_d = 300$.

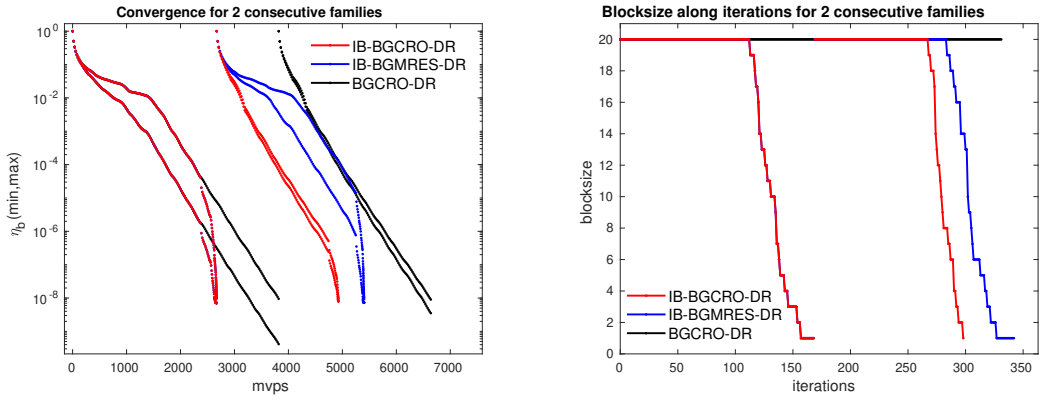

Figure 3: Comparison history for Section 5.3. IB-BGCRO-DR with BGCRO-DR and IB-BGMRES-DR by solving Matrix 1 ($p = 20$, $m_d = 300$ and $k = 30$). Left: convergence histories of the largest/smallest backward errors $\eta_{b^{(i)}}$ at each $mvps$ for 2 consecutive families. Right: varying blocksize along iterations.

In the left plot of Figure 3 we display the convergence histories for solving two consecutive families with η_b-based stopping criterion. Several observations can be made. Because IB-BGMRES-DR, IB-BGCRO-DR and BGCRO-DR do not have a deflation space to start with for the first family, the convergence histories of these three solvers overlap as long as the IB mechanism does not detect any partial convergence. After this first IB-point, the convergence rate of IB-BGCRO-DR and IB-BGMRES-DR becomes faster (in terms of $mvps$) than that of BGCRO-DR, and the former two convergence histories mostly overlap as the two IB solvers remain mathematically equivalent. For the second and subsequent families, the capability to start with a deflation space shows its benefit for BGCRO-DR and IB-BGCRO-

DR. It is because IB-BGMRES-DR needs a few restarts to capture this spectral information again and refines it in its subsequent search spaces; eventually it exhibits a convergence rate similar to the BGCRO-DR counterpart. For the sake of comparison and to illustrate the benefit of the IB mechanism we also display the converge histories of BGCRO-DR which always requires more $mvps$ compared to its IB counterpart. Those extra $mvps$ mostly concur to improve the solution quality for some right-hand sides beyond the targeted accuracy.

To visualize the effect of the IB mechanism, we also report in the right plot of Figure 3 the size of search space expansion as a function of the iterations. Because BGCRO-DR does not implement the IB mechanism, its search space is increased by $p = 20$ at each iteration. For the other two block IB-solvers, the block size monotonically decreases down to 1. Note that the IB mechanism is implemented in initial (least squares) residual block in IB-BGCRO-DR, thus its block size does not jump back to the original block size p at restart. By construction, IB-BGMRES-DR implements the IB mechanism at restart so that the same observation applies.

Number of families	Method	$mvps$	its
2	BGCRO-DR	6640	332
	IB-BGMRES-DR	5404	343
	IB-BGCRO-DR	**4928**	**299**
20	BGCRO-DR	56940	2847
	IB-BGMRES-DR	53772	3454
	IB-BGCRO-DR	**45652**	**2637**

Table 2: Numerical results in both terms of $mvps$ and its for Section 5.3 with Matrix 1 ($p = 20$, $m_d = 300$ and $k = 30$).

A summary of the $mvps$ and the number of block iterations (referred to as its) is given in Table 2 that shows the benefit of using IB-BGCRO-DR.

Note that we introduced inexact breakdown (IB) detection in the initial residual block for the proposed solver as described in Section 4.1, what would happen if we skip it for the first initial residual block ? Let's denote the solver with IB detection after the initial residual block as IBa-BGCRO-DR, where IBa stands for carrying out Inexact Breakdown after initial iteration (or without IB detection in the initial residual block), for contrasting with IB-BGCRO-DR that with IB detection in initial residual block thus also with the updating right-hand sides of least-squares problem as shown in Equation (41). From the pseudocode of IB-BGCRO-DR for slowly-changing left-hand sides with massive number of right-hand sides as shown in Algorithm 2, the corresponding pseudocode for IBa-BGCRO-DR could be deduced similarly by letting all the columns of the initial residual block be the an initial Arnoldi basis $\mathbb{V}_1^{new}$ with p columns thus P_0^{new} is empty within such case, and by replacing the varying right-hand sides Λ_j shown in Proposition 4 into a one that with simple version as $\Lambda_j = \left[0_{p\times k}, \Lambda_1^T, 0_{p\times n_j}\right]^T$. Figure 4 displays the results of adding the performance of IBa-BGCRO-DR to Figure 3 in Section 5.3 to illustrate the benefit of introducing IB in the initial residual block, i.e., reduce $mvps$ by avoiding block-size jumps back to the original block-size p at restart.

5.4 Subspace expansion governed by the convergence criterion $\eta_{A,b}$

In this section we show the capability of the novel subspace expansion policy to drive the individual backward errors $\eta_{A,b}$ down to different accuracies and its benefit with respect to the original BGCRO-DR method. In Figure 5, we display the convergence histories of the IB and IB-free method for three different convergence thresholds, from the less stringent on the left to the most stringent on the right. We can firstly

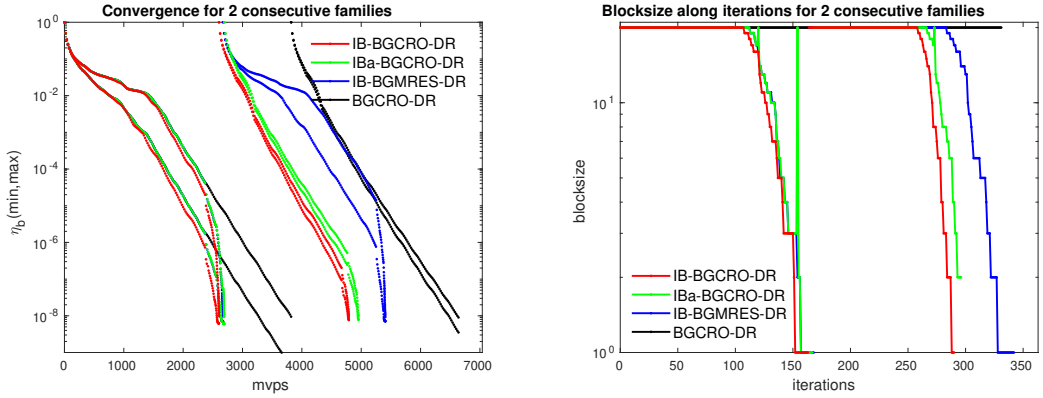

Figure 4: Comparison of IB-BGCRO-DR with IBa-BGCRO-DR, BGCRO-DR and IB-BGMRES-DR by solving bidiagonal Matrix 1 ($p = 20$, $m_d = 300$ and $k = 30$). Left: convergence histories of the largest/smallest backward errors $\eta_{b^{(i)}}$ at each $mvps$ for 2 consecutive families. Right: varying blocksize along iterations.

observe that the first iteration, where the IB mechanism starts to act, depends on the targeted accuracy as it can have been expected from the associated threshold on the singular values of the least squares residual. The second interesting observation is that IB-BGCRO-DR is able to decrease $\eta_{A,b}$ down to a very low

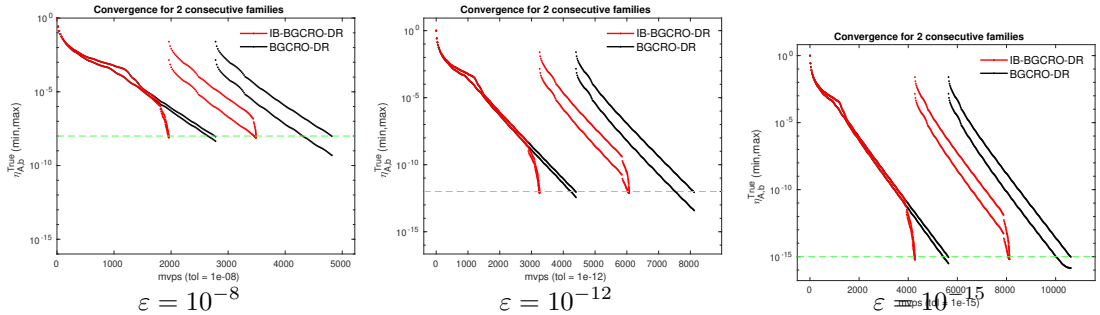

$\varepsilon = 10^{-8}$ $\varepsilon = 10^{-12}$ $\varepsilon = 10^{-15}$

Figure 5: Convergence histories of the largest/smallest $\eta_{A,b^{(i)}}(x_j^{(i)})$ at each $mvps$ for 2 consecutive families for Section 5.4 with different convergence thresholds. Comparison of IB-BGCRO-DR with BGCRO-DR by solving Matrix 1 ($p = 20$, $m_d = 300$ and $k = 30$).

value close to the machine epsilon, that is $\mathcal{O}(10^{-16})$. This latter result mostly reveals the orthogonality quality of the residual space basis computed by the Modified Gram-Schmidt with Ruhe (MGS-Ruhe) [20] variant of the block Arnoldi implementation and the re-orthogonalization between all the columns of the recycling subspace C_k and the initial block Arnoldi basis at restart, that both ensure the least squares residual norms to be quite close to the linear system residual ones. This latter fact ensures the relevance of the space expansion policy, that monitors the linear system residual norms through the least squares residual ones. To illustrate the orthonormal quality of the basis $\widehat{\mathscr{V}}_{j+1} = \left[C_k, \mathscr{V}_j, [P_{j-1}, \widetilde{W}_j]\right]$, we display in Figure 6 the loss of orthogonality along $mvps$ that is defined by

$$\text{Loss-Orth} = \left\| \widehat{\mathscr{V}}_{j+1}^H \widehat{\mathscr{V}}_{j+1} - I_{j+1} \right\|. \tag{45}$$

In a quite similar manner to MGS-Ruhe-GMRES, that is backward-stable [13], it can be observed that the loss of orthogonality mostly appears when the solutions of the linear systems converge. Note that without the re-rothogonalization at restart, the loss of orthogonality tends to be accumulated along restart which prevents the value of Loss-Orth to be close to the machine epsilon. Refer to Figure 7 for the corresponding results without applying re-orthogonalization to all the columns of $[C_k, [\mathbb{V}_1, P_0]]$ at restart.

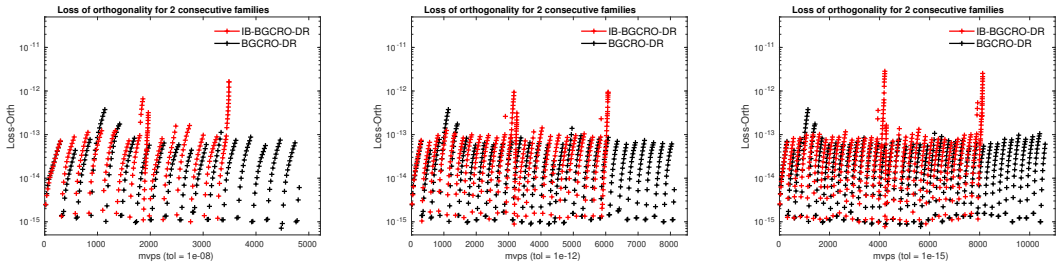

Figure 6: Loss-Orth defined in Equation (45) of GCRO-variants with stopping criterion based on $\eta_{A,b^{(i)}}(x_j^{(i)})$ at each $mvps$ for 2 consecutive families for Section 5.4 with different convergence thresholds. Comparison IB-BGCRO-DR with BGCRO-DR for solving Matrix 1 ($p = 20$, $m_d = 300$ and $k = 30$).

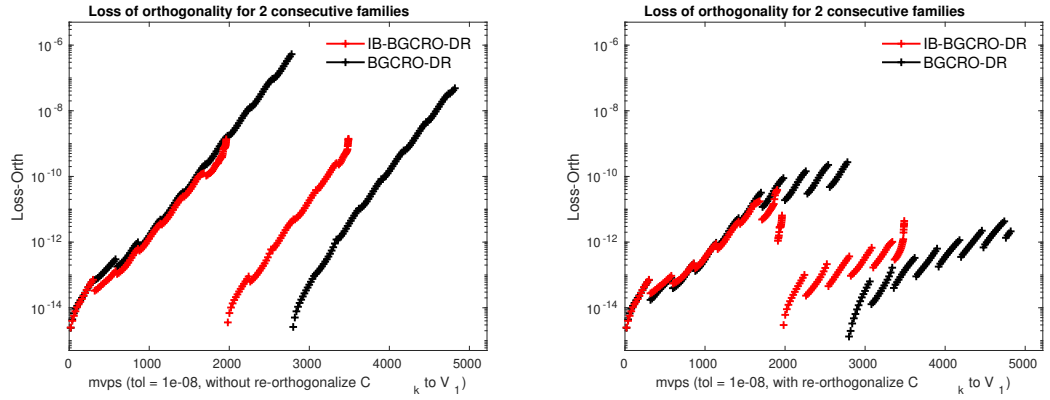

Figure 7: Loss-Orth defined in Equation (45) of GCRO-variants with stopping criterion $\eta_{A,b^{(i)}}(x_j^{(i)}) \leq 10^{-8}$ at each $mvps$ for 2 consecutive families for Section 5.4 with or without re-orthogonalizing C_k to $\mathbb{V}_1$ ($\mathcal{V}_1$) by MGS at restart of (IB-)BGCRO-DR. * Note the above mentioned re-orthogonalizing C_k to $\mathbb{V}_1$ cannot ensures the re-orthogonality in all the columns of C_k (or $\mathbb{V}_1$) thus cannot obtain results as shown in left plot of Figure 6 that with applying re-orthogonalization to all the columns of $[C_k, [\mathbb{V}_1, P_0]]$ at restart.

5.5 Subspace expansion policy for individual convergence thresholds for η_b

To illustrate this feature, we consider a family of p right-hand sides and a convergence threshold 10^{-4} for the first $p/2$ right-hand sides and 10^{-8} for the last $p/2$ ones. As an estimate of the computational benefit of this feature, we also compare with calculations where all the right-hand sides are solved with the most stringent accuracy, that is 10^{-8}. We display in the left part of Figure 8, the convergence histories for 3 successive families. The variant that controls the individual threshold is denoted as IB-BGCRO-DR-VA, where VA stands for Variable Accuracy. It can be seen that the numerical feature works well and that

the envelope of the backward errors has the expected shape, that is, the minimum backward error goes down to 10^{-8} while the maximum one (associated with the first $p/2$ solutions) only goes down to 10^{-4}. If we compare the convergence histories of IB-BGCRO-DR and IB-BGCRO-DR-VA, it can be seen that the slope of IB-BGCRO-DR-VA is deeper than that of IB-BGCRO-DR once the first $p/2$ solutions have converged; after this point IB-BGCRO-DR-VA somehow focuses on the new directions (produced by $mvps$ given for the x-axis) to reduce the residual norms of the remaining $p/2$ solutions that have not yet converged. The right plot of Figure 8 shows the computational gain induced by the individual control of the accuracy compared to the situation where all the right-hand sides would have been solved to the most stringent one if this feature had not been designed. In this case the individual monitoring of the convergence saves around 45 % of $mvps$ on this example. Those results are summarized in Table 3.

We refer to Figure 11 and Table 8 of Appendix F for an illustration of extending such individual control to the block solver IB-BGMRES-DR that can also accommodate this feature.

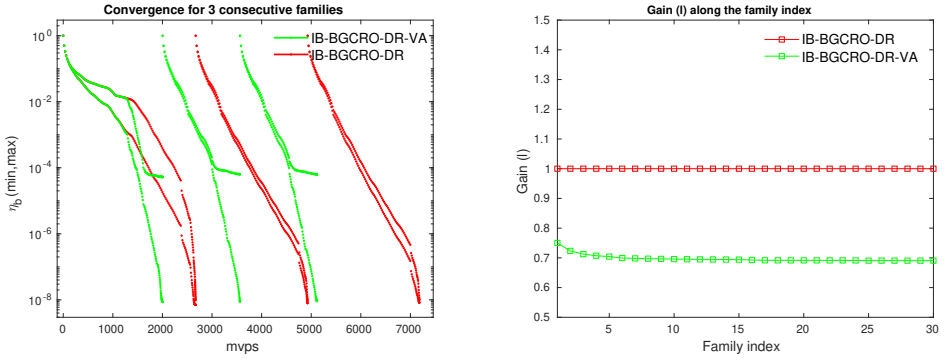

Figure 8: Comparison of IB-BGCRO-DR to IB-BGCRO-DR-VA for Section 5.5 with Matrix 1 ($p = 20$, $m_d = 300$ and $k = 30$). Left: convergence histories of the largest/smallest backward errors $\eta_{b^{(i)}}$ at each $mvps$ for 3 consecutive families. Right: Gain (ℓ) defined in Equation (43) of IB-BGCRO-DR-VA to IB-BGCRO-DR versus family index.

Number of families	Method	$mvps$	its
3	IB-BGCRO-DR	7182	428
	IB-BGCRO-DR-VA	**5119**	**395**
30	IB-BGCRO-DR	68263	3932
	IB-BGCRO-DR-VA	**47143**	**3566**

Table 3: Numerical results of IB-BGCRO-DR with fixed/varying accuracy for each right-hand side in terms of $mvps$ and its for Section 5.5, where the coefficient matrix is Matrix 1 with $p = 20$, $m_d = 300$ and $k = 30$.

5.6 Expansion policy governed by computational performance

As discussed in Section 3.3, only a subset of the candidate directions exhibited by the IB mechanism can be eventually selected to expand the search space at the next block iteration; we denote this maximum size p^{CB} and refer to this variant as IB-BGCRO-DR-CB where the CB stands for Computational Blocking. In Table 4 we show the effect of this algorithmic parameter on $mvps$ and its for the solutions of 3 and 30 families with Matrix 1 when p^{CB} varies from 1 to 15 for a number of right-hand sides $p = 20$. Generally, the smaller p^{CB} is, the smaller $mvps$, but the larger its. While reported only on one example

this trend has been observed in all our numerical experiments. Depending on the computational efficiency or cost of the $mvps$ with respect to the computational weight of the least-squares problem and SVD of the scaled least squares residual, this gives opportunities to monitor the overall computational efficiency of the complete solution.

Number of families	Method	$mvps$	its
3	IB-BGCRO-DR	7182	**428**
	IB-BGCRO-DR-CB ($p^{CB} = 15$)	**6934**	467
	IB-BGCRO-DR-CB ($p^{CB} = 10$)	6941	668
	IB-BGCRO-DR-CB ($p^{CB} = 5$)	6968	1312
	IB-BGCRO-DR-CB ($p^{CB} = 1$)	6966	6444
30	IB-BGCRO-DR	68262	**3932**
	IB-BGCRO-DR-CB ($p^{CB} = 15$)	**65364**	4303
	IB-BGCRO-DR-CB ($p^{CB} = 1$)	65823	60836

Table 4: Numerical results of IB-BGCRO-DR and IB-BGCRO-DR-CB for $p^{CB} = 1, 5, 10, 15$ in terms of $mvps$ and its for Section 5.6, where the coefficient matrix is Matrix 1 with $p = 20$, $m_d = 300$ and $k = 30$.

Similar to previous subsections, we notice that this subspace expansion policy also applies to IB-BGMRES-DR and we refer to Figure 12 and Table 9 of Appendix G for an illustration.

5.7 Behavior on sequences of slowly-varying left-hand sides problems

The example used in this section is from a finite element fracture mechanics problem in the field of Fatigue and Fracture of Engineering Components (denoted as *FFEC* collection), which is fully documented in [15, Section 4.1]. Over 2000 linear systems of size 3988×3988 from *FFEC* collection need to be solved in order to capture the fracture progression, and among them 151 linear systems $400 - 550$ representing a typical subset of the fracture progression in which many cohesive elements break are examined in [15]. The solutions of these linear systems have been investigated using both GCRO-DR and GCROT (generalized conjugate residual with inner orthogonalization and outer truncation), and we refer to [7] for a comprehensive experimental analysis. For our numerical experiments we borrow the ten linear systems numbered $400 - 409$ from this *FFEC* collection. For each set of linear system we select the matrix and the corresponding right-hand sides that we expand to form a block of $p = 20$ by appending random linearly independent vectors.

We display the convergence histories for solving the first 3 consecutive families of such linear systems in the left plot of Figure 9. For the solution of the first linear system, the observations on the IB and DR mechanisms discussed in Section 5.3 apply. Even though the coefficient matrix has changed, the recycling spectral information computed for the previous family still enables a faster convergence at the beginning of the solution of the next one. Specifically, for the solution of the first family the convergence histories of the two methods fully overlap until the first inexact breakdown occurs, as until this step the two methods are the same. From the initial slope of the subsequent families, it can be seen that the sequence of matrices are close enough to ensure that the recycled space from one system to the next still makes benefit to the convergence. The benefit of the IB mechanism is also illustrated on that example as IB-BGCRO-DR still outperforms BGCRO-DR. The overall benefit in term of $mvps$ saving is illustrated in the right plot on a sequence of 10 linear systems, where the saving is more than 65 % with respect to BGCRO-DR. Corresponding results are summarized in Table 5.

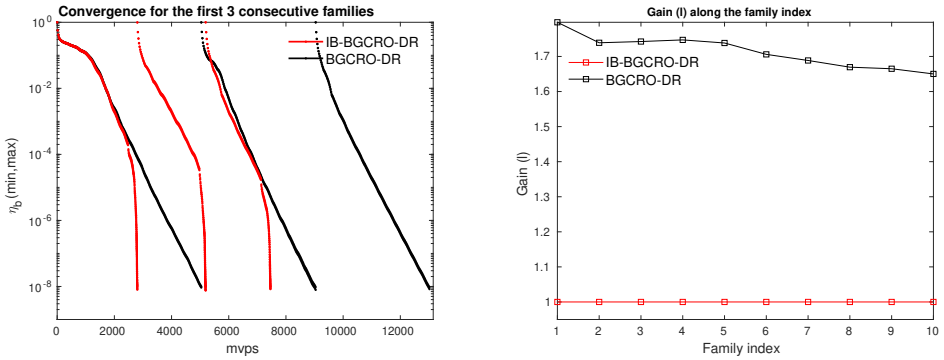

Figure 9: Convergence results of IB-BGCRO-DR and BGCRO-DR on a sequence of slowly-changing left-hand sides described in Section 5.7, where the coefficient matrices are built on FFEC with $p = 20$, $m_d = 300$ and $k = 15$.

Number of families	Method	$mvps$	its
3	BGCRO-DR	13050	651
	IB-BGCRO-DR	**7489**	**540**
10	BGCRO-DR	39935	1990
	IB-BGCRO-DR	**24200**	**1658**

Table 5: Numerical results in terms of $mvps$ and its for Section 5.7 with $p = 20$, $m_d = 300$ and $k = 15$.

5.8 A variant suited for flexible preconditioning

In this section, we illustrate the numerical behavior of the flexible variant IB-BFGCRO-DR that we have derived in Section 2.5 and make comparison with closely related variants namely BFGCRO-DR (a straightforward block extension of FGCRO-DR [4]).

We consider a representative quantum chromodynamics (QCD) matrix from the University of Florida sparse matrix collection [5]. It is the conf5.4-00l8x8-0500 matrix denoted as B_{QCD} of size 49152×49152 with the critical parameter $\kappa_c = 0.17865$ as a model problem. Thirty families of linear systems are constructed that are defined as $A^{(\ell)} = I - \kappa_c(\ell) B_{\text{QCD}}$ with $0 \leq \kappa_c(\ell) < \kappa_c$ and $\ell = 1, 2, \ldots, 30$. We use the MATLAB function **linspace**$(0.1780, 0.1786, 30)$ to generate the parameters $\kappa_c(\ell)$ for a sequence of matrices and observe that those matrices have the same eigenvectors associated with shifted eigenvalues. A sequence of $p = 12$ successive canonical basis vectors are chosen to be the block of right-hand sides for a given left-hand side matrix following [15, Section 4.3] so that the complete set of the right-hand sides for the ℓ linear systems reduces to the first $p \times \ell$ columns of the identity matrix. This choice could be supported by the fact that the problem of numerical simulations of QCD on a four-dimensional space-time lattice for solving QCD ab initio (cf. [15, Section 4.3]) has a 12×12 block structure, and then a system with 12 right-hand sides related to a single lattice site is often of interest to solve.

The flexible preconditioner is defined by a 32-bit incomplete $LU(0)$ factorization of the matrix involved in the linear system. In a 64-bit calculation framework, the preconditioning consists in casting the set of directions to be preconditioned in 32-bit format, performing the forward/backward substitution in 32-bit calculation and casting back the solutions in 64-bit arithmetic. The rounding applied to the vectors has a nonlinear effect that makes the preconditioner nonlinear.

For those experiments, we attempt to favor the recycling of the space, because the matrices share the same invariant space, so that we choose a relative large value for k that is $k = m_d/2$. We report in the

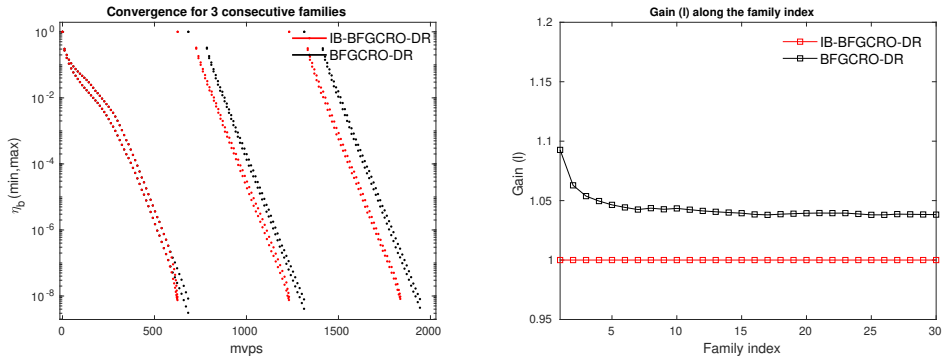

Figure 10: Behavior of the BGCRO-DR-solvers with flexible preconditioner on families of QCD matrices described in Section 5.8 with $p = 12$, $m_d = 180$ and $k = 90$. Left: convergence histories of the largest/smallest backward errors $\eta_{b(i)}$ at each $mvps$ for 3 consecutive families. Right: Gain (l) of the block methods with respect to IB-BFGCRO-DR along family index.

Number of families	Method	$mvps$	its
3	BFGCRO-DR	1944	**147**
	IB-BFGCRO-DR	**1838**	148
30	BFGCRO-DR	18774	**1347**
	IB-BFGCRO-DR	**18054**	1350

Table 6: Numerical results in terms of $mvps$ and its for Section 5.8 with $p = 12$, $m_d = 15 \times p = 180$ and $k = 90$.

left plot of Figure 10, the convergence histories of the two flexible block variants. Similarly to what has already been observed previously the convergences are very similar on the first family and only differ when the IB mechanism becomes active mostly in the last restart. For the second and third families, one can see that IB-BFGCRO-DR and BFGCRO-DR have identical convergence speed. One can observe a shift in the convergence histories between the end of the solution of one family and the beginning of the next one for both IB-BFGCRO-DR and BFGCRO-DR. This shift is due to the extra k $mvps$ that have to be performed when the matrix changes in order to adapt the recycling space as follows

1. compute $A^{(\ell+1)}U_k^{(\ell)} = \tilde{C}_k$
2. compute the reduced QR factorization of $\tilde{C}_k = C_k^{(\ell+1)}R$
3. update the basis of the deflation space $U_k^{(\ell+1)} = U_k^{(\ell)}R^{-1}$ so that $A^{(\ell+1)}U_k^{(\ell+1)} = C_k^{(\ell+1)}$.

Because k is large, we can clearly see this shift in the left plot of Figure 10. For this parameter selection in this section, it can be noticed that the dominating effect on the convergence improvement is due to the space recycling and not the IB mechanism. This observation is highlighted in the right plot of Figure 10, where the benefit of using IB-BFGCRO-DR rather than BFGCRO-DR does diminish when compared to previous experiments and is only about 4%. Numerical details are summarized in Table 6.

6 Concluding remarks

In this paper, we develop a new variant of block GCRO-DR method denoted as IB-BGCRO-DR that inherits the appealing genes of its two parents [15, 19]. First, it inherits the capabilities to speed up the convergence rate when solving sequences of linear systems by recycling spectral information from one family to the next. Second, the extended search space expansion policy enabled by the so-called inexact breakdown allows us to focus on the convergence by considering only the most important directions. Along this line, we introduce stopping-criterion driven search space expansion polices that enable us to ensure that a prescribed threshold used for inexact breakdown detection will eventually be reached for a prescribed stopping criterion based on a backward error. While introduced in the block GCRO context, those policies apply to any block minimum residual norm approach that relies on an Arnoldi-like relation and includes both block GMRES and GCRO variants. In exact arithmetic, these policies exploit the close link between the least squares residual and the linear systems residual, which is guaranteed by the orthonormal basis of the residual space. Through numerical experiments, we show that MGS-Ruhe [20] variant of the block Arnoldi algorithm and re-orthogonalization between the columns of recycling space and initial block Arnoldi basis at restart seems to generate good enough orthonormal basis to ensure that such a property does also hold in finite precision calculation. To theoretically establish that this class of algorithms is backward stable following ideas from [13] would be the topic of a future research work. To comply with mixed-precision calculation, the flexible preconditioning variant is also proposed, which would be of interest for emerging computing platforms where mixed-precision calculation could be a way to reduce data movement that is foreseen as one of the major bottleneck to reach high performance.

Acknowledgments

We would like to thank Matthieu Simonin (who developed a C++ implementation of the solver - available on https://gitlab.inria.fr/solverstack/fabulous/ - in the framework of the PRACE 6IP project) for his reading and comments on earlier version of this document. The second author is supported by Science Challenge Project (TZ2016002-TZZT2019-B1.4), NSFC (12071062, 61772003), Key Projects of Applied Basic Research in Sichuan Province (Grant No. 2020YJ0216), and Science Strength Promotion Programme of UESTC.

Finally, we thank the anonymous referees, whose valuable and pertinent comments helped us not only to improve the readability of the article but also to enrich its scientific content.

References

[1] E. Agullo, L. Giraud, and Y.-F. Jing. Block GMRES method with inexact breakdowns and deflated restarting. *SIAM J. Matrix Anal. Appl.*, 35(4):1625–1651, 2014.

[2] H. Calandra, S. Gratton, R. Lago, X. Vasseur, and L. M. Carvalho. A modified block flexible GMRES method with deflation at each iteration for the solution of non-Hermitian linear systems with multiple right-hand sides. *SIAM J. Sci. Comput.*, 35:S345–S367, 2013.

[3] L. M. Carvalho, S. Gratton, R. Lago, and X. Vasseur. A flexible generalized Conjugate Residual method with inner orthogonalization and deflated restarting. Technical Report TR/PA/10/10, CERFACS, Toulouse, France, 2010.

[4] L. M. Carvalho, S. Gratton, R. Lago, and X. Vasseur. A flexible generalized conjugate residual method with inner orthogonalization and deflated restarting. *SIAM J. Matrix Anal. Appl.*, 32:1212–1235, 2011.

[5] T. A. Davis and Y. Hu. The University of Florida Sparse Matrix Collection. *ACM Trans. Math. Softw.*, 38:1:1–1:25, 2011.

[6] E. de Sturler. Nested Krylov methods based on GCR. *J. Comput. Appl. Math.*, 67:15–41, 1996.

[7] E. de Sturler. Truncation strategies for optimal Krylov subspace methods. *SIAM J. Numer. Anal.*, 36:864–889, 1999.

[8] L. Giraud, S. Gratton, X. Pinel, and X. Vasseur. Flexible GMRES with deflated restarting. *SIAM J. Sci. Comput.*, 32:1858–1878, 2010.

[9] M. H. Gutknecht. Block Krylov space methods for linear systems with multiple right-hand sides: An introduction. In I. S. Duff, A. H. Siddiqi, and O. Christensen, editors, *Modern Mathematical Models, Methods and Algorithms for Real World Systems*, pages 420–447. Anamaya Publishers, New Delhi, India, 2006.

[10] R. B. Morgan. A restarted GMRES method augmented with eigenvectors. *SIAM J. Matrix Anal. Appl.*, 16:1154–1171, 1995.

[11] R. B. Morgan. GMRES with deflated restarting. *SIAM J. Sci. Comput.*, 24(1):20–37, 2002.

[12] R. B. Morgan. Restarted block GMRES with deflation of eigenvalues. *Appl. Numer. Math.*, 54(2):222–236, 2005.

[13] C. C. Paige, M. Rozloznik, and Z. Strakos. Modified Gram-Schmidt (MGS), Least Squares, and Backward Stability of MGS-GMRES. *SIAM J. Matrix Anal. Appl.*, 28(1):264–284, 2006.

[14] M. L. Parks. The Iterative Solution of a Sequence of Linear Systems Arising from Nonlinear Finite Element Analysis. Ph.D. Dissertation UIUCDCS-R-2005-2497, University of Illinois at Urbana-Champaign, 2005.

[15] M. L. Parks, E. de Sturler, G. Mackey, D.D. Johnson, and S. Maiti. Recycling Krylov subspaces for sequences of linear systems. *SIAM J. Sci. Comput.*, 28(5):1651–1674, 2006.

[16] M. L. Parks and K. M. Soodhalter. Block GCRO-DR. in Belos package of the Trilinos C++ Library, 2011.

[17] M. L. Parks, K. M. Soodhalter, and D. B. Szyld. A block recycled GMRES method with investigations into aspects of solver performance, 2016. http://arxiv.org/abs/1604.01713.

[18] L. G. Ramos, R. Kehl, and R. Nabben. Projections, deflation, and multigrid for nonsymmetric matrices. *SIAM J. Matrix Anal. Appl.*, 41(1):83–105, 2020.

[19] M. Robbé and M. Sadkane. Exact and inexact breakdowns in the block GMRES method. *Linear Algebra Appl.*, 419:265–285, 2006.

[20] A. Ruhe. Numerical aspects of Gram-Schmidt orthogonalization of vectors. *Numer. Linear Algebra Appl.*, 52(53):591–601, 1983.

[21] Y. Saad and M. H. Schultz. GMRES: A generalized minimal residual algorithm for solving nonsymmetric linear systems. *SIAM J. Sci. Stat. Comput.*, 7:856–869, 1986.

[22] K. Soodhalter. Krylov Subspace Methods with Fixed Memory Requirements: Nearly Hermitian Linear Systems and Subspace Recycling. Ph.D. dissertation, Temple University, 2012.

[23] D.-L. Sun, B. Carpentieri, T.-Z. Huang, and Y.-F. Jing. A spectrally preconditioned and initially deflated variant of the restarted block GMRES method for solving multiple right-hand sides linear systems. *Internat. J. Mech. Sci.*, 144:775–787, 2018.

[24] D.-L. Sun, T.-Z. Huang, B. Carpentieri, and Y.-F. Jing. Flexible and deflated variants of the block shifted GMRES method. *J. Comput. Appl. Math.*, 345:168–183, 2019.

[25] D.-L. Sun, T.-Z. Huang, B. Carpentieri, and Y.-F. Jing. A new shifted block GMRES method with inexact breakdowns for solving multi-shifted and multiple right-hand sides linear systems. *J. Sci. Comput.*, 78:746–769, 2019.

[26] D.-L. Sun, T.-Z. Huang, Y.-F. Jing, and B. Carpentieri. A block GMRES method with deflated restarting for solving linear systems with multiple shifts and multiple right-hand sides. *Numer. Linear Algebra Appl.*, 25, 2018. e2148. https://doi.org/10.1002/nla.2148.

[27] A. Tajaddini, G. Wu, F. S. Movahed, and N. Azizizadeh. Two new variants of the simpler block GMRES method with vector deflation and eigenvalue deflation for multiple linear systems. *J. Sci. Comput.*, 86, 2021.

[28] Y.-F. Xiang, Y.-F. Jing, and T.-Z. Huang. A new projected variant of the deflated block conjugate gradient method. *J. Sci. Comput.*, 80:1116–1138, 2019.

[29] F. Xue and H. C. Elman. Fast inexact subspace iteration for generalized eigenvalue problems with spectral transformation. *Linear Algebra Appl.*, 435:601–622, 2011.

A Other two alternatives to compute the approximate eigen-information

Proposition 5. *(Strategy A [3]) At the end of a cycle of the IB-BFGCRO-DR algorithm, if the deflation space is built on the harmonic-Ritz vectors* $g_i \in \mathrm{span}(\widehat{\mathscr{Z}_m})$ *of* A *with respect to* $\widehat{\mathscr{Z}_m} = [U_k \quad \mathscr{Z}_m] \in \mathbb{C}^{n\times(k+n_m)}$:

1. *The harmonic-Ritz pairs* $(\theta_i, \widehat{\mathscr{Z}_m} g_i)$ *for the each restart satisfy*

$$\underline{\mathscr{F}}_m^H \underline{\mathscr{F}}_m g_i = \theta_j \underline{\mathscr{F}}_m^H \widehat{\mathscr{V}}_{m+1}^H \widehat{\mathscr{Z}_m} g_i, \quad \textit{for } 1 \le i \le n_m, \tag{46}$$

where

$$\widehat{\mathscr{V}}_{m+1}^H \widehat{\mathscr{Z}_m} = \begin{bmatrix} C_k^H U_k & C_k^H \mathscr{Z}_m \\ \mathscr{V}_m^H U_k & \mathscr{V}_m^H \mathscr{Z}_m \\ \begin{bmatrix} P_{m-1}^H U_k \\ \widetilde{W}_m^H U_k \end{bmatrix} & \begin{bmatrix} P_{m-1}^H \mathscr{Z}_m \\ \widetilde{W}_m^H \mathscr{Z}_m \end{bmatrix} \end{bmatrix} \in \mathbb{C}^{(k+n_m+p)\times(k+n_m)}. \tag{47}$$

2. *At restart, if* $G_k = [g_1, \ldots, g_k]$ *is associated with the* k *targeted eigenvalues, the matrices* U_k^{new} *and* C_k^{new} *to be used for the next cycle are defined by*

$$U_k^{new} = \widehat{\mathscr{Z}_m} G_k R^{-1} = [U_k, \mathscr{Z}_m] G_k R^{-1}, \tag{48}$$

$$C_k^{new} = \widehat{\mathscr{V}}_{m+1} Q = [C_k, \mathscr{V}_m, P_{m-1}, \widetilde{W}_m] Q, \tag{49}$$

where Q *and* R *are the factors of the reduced* QR*-factorization of* $\underline{\mathscr{F}}_m G_k$ *that ensures* $AU_k^{new} = C_k^{new}$ *with* $(C_k^{new})^H C_k^{new} = I_k$.

3. *The residual at restart* $R_1^{new} = R_m^{old} = B - AX_1^{new}$ *with* $X_1^{new} = X_m^{old}$ *is orthogonal to* C_k^{new}.

Proof. The proofs basically relay on some matrix computations as shortly described below:

- According to Definition 1, each harmonic-Ritz pair $(\theta_i, \widehat{\mathscr{Z}_m} g_i)$ satisfies

$$\forall w \in \mathrm{Range}(A\widehat{\mathscr{Z}_m}) \quad w^H (A\widehat{\mathscr{Z}_m} g_i - \theta_i \widehat{\mathscr{Z}_m} g_i) = 0, \tag{50}$$

  which equivalently becomes

$$(A\widehat{\mathscr{Z}_m})^H (A\widehat{\mathscr{Z}_m} g_i - \theta_i \widehat{\mathscr{Z}_m} g_i) = 0. \tag{51}$$

  Using Equation (26) leads to

$$\left(\widehat{\mathscr{V}}_{m+1} \underline{\mathscr{F}}_m\right)^H \left(\widehat{\mathscr{V}}_{m+1} \underline{\mathscr{F}}_m g_i - \theta_i \widehat{\mathscr{Z}_m} g_i\right) = 0. \tag{52}$$

  Because $\widehat{\mathscr{V}}_{m+1} = [C_k, \mathscr{V}_m, [P_{m-1}, \widetilde{W}_m]]$ generated at the end of cycle is orthonormal, Equation (52) becomes

$$\underline{\mathscr{F}}_m^H \underline{\mathscr{F}}_m g_i - \theta_i \underline{\mathscr{F}}_m^H \widehat{\mathscr{V}}_{m+1}^H \widehat{\mathscr{Z}_m} g_i = 0,$$

  which is the same as formulation (46).

- Let Q and R be the factors of the reduced QR-factorization of $\underline{\mathscr{F}}_m G_k$ and multiply by G_k on the both sides of Equation (26). It leads to $A\widehat{\mathscr{Z}_m} G_k = \widehat{\mathscr{V}}_{m+1} \underline{\mathscr{F}}_m G_k = \widehat{\mathscr{V}}_{m+1} QR$, that is equivalent to $A\widehat{\mathscr{Z}_m} G_k R^{-1} = \widehat{\mathscr{V}}_{m+1} \underline{\mathscr{F}}_m G_k R^{-1} = \widehat{\mathscr{V}}_{m+1} Q$ that concludes the proof as $\widehat{\mathscr{V}}_{m+1} Q$ is the product of two matrices with orthonormal columns so are its columns.

- The same process for proving Corollary 1.

□

Proposition 6. *(Strategy B [3]) At the end of a cycle of the IB-BFGCRO-DR algorithm, if the deflation space is built on the harmonic-Ritz vectors* $g_i \in \mathrm{span}(\widehat{\mathscr{V}}_m)$ *of* $A\widehat{\mathscr{Z}}_m\widehat{\mathscr{V}}_m^H$ *with respect to* $\widehat{\mathscr{V}}_m = [C_k \quad \mathscr{V}_m] \in \mathbb{C}^{n\times(k+n_m)}$ *:*

1. *The harmonic-Ritz pairs* $(\theta_i, \widehat{\mathscr{V}}_m g_i)$ *for the each restart satisfy*

$$\underline{\mathscr{F}}_m^H \underline{\mathscr{F}}_m g_i \quad = \quad \theta_i \, \mathscr{F}_m^H g_i \quad \text{for } 1 \le i \le n_m, \tag{53}$$

2. *At restart, if* $G_k = [g_{i_1}, \ldots, g_{i_k}]$ *is associated with the* k *targeted eigenvalues, the matrices* U_k^{new} *and* C_k^{new} *to be used for the next cycle are defined by*

$$U_k^{new} \quad = \quad \widehat{\mathscr{Z}}_m G_k R^{-1} = [U_k, \mathscr{Z}_m] G_k R^{-1}, \tag{54}$$
$$C_k^{new} \quad = \quad \widehat{\mathscr{V}}_{m+1} Q = [C_k, \mathscr{V}_m, P_{m-1}, \widetilde{W}_m] Q, \tag{55}$$

   where Q *and* R *are the factors of the reduced* QR*-factorization of* $\underline{\mathscr{F}}_m G_k$ *that ensures* $AU_k^{new} = C_k^{new}$ *with* $(C_k^{new})^H C_k^{new} = I_k$*.*

3. *The residual at restart* $R_1^{new} = R_m^{old} = B - AX_1^{new}$ *with* $X_1^{new} = X_m^{old}$ *is orthogonal to* C_k^{new}*.*

Proof. Given the proof essentially follows the same arguments as the ones developed for Proposition 5 or 2, the details are omitted here. □

Although the Strategy A depicted in Proposition 5 is the most efficient way among the possible three strategies described in [3] for approximating the eigen-information of the coefficient matrix A, the computational cost of the last n_m columns of $\widehat{\mathscr{V}}_{m+1}^H \widehat{\mathscr{Z}}_m$ as shown in the right-hand side of Equation (47) is too heavy especially with larger n_m. Therefore, another possible alternatives are considered to reduce the computational cost of solving such general eigen-solving problem. Inspired from the way of computing eigen-information under the context of flexible GMRES with deflated restarting (FGMRES-DR) as shown in [8, Proposition 1], Strategy B shown in Proposition 6 is described for the IB-BFGCRO-DR, while which turns out to be not that suitable under the GCRO-DR context by numerical results shown in Table 7. Thus, the Strategy C is devised and described in Proposition 2, which has the same sense as Strategy A but with a lower computational cost of solving the general eigen-solving problem as shown in Equation (27). From Table 7, it is easy to observed that the numerical result of IB-BFGCRO-DR with Strategy C is approximate to that with Strategy A through the later one costs the fewest $mvps$ and its.

Number of families	Method	$mvps$	its
3	IB-BFGCRO-DR (Strategy A)	**1807**	**144**
	IB-BFGCRO-DR (Strategy B)	2074	177
	IB-BFGCRO-DR (Strategy C)	1838	148

Table 7: Numerical results of IB-BFGCRO-DR with three kinds of strategies in terms of $mvps$ and its, in which the involving parameters for QCD matrix are set to be $p = 12$, $m_d = 15 \times p = 180$ and $k = 90$.

B Proof of Proposition 2

Proof. The proofs basically relay on some matrix computations as shortly described below:

- According to Definition 1, each harmonic-Ritz pair $(\theta_i, \mathcal{W}_m g_i)$ satisfies

$$\forall w \in \mathrm{Range}(A\widehat{\mathscr{Z}_m}\mathcal{W}_m^{\dagger}\mathcal{W}_m) \quad w^H\,(A\widehat{\mathscr{Z}_m}\mathcal{W}_m^{\dagger}\mathcal{W}_m g_i - \theta_i\,\mathcal{W}_m g_i) = 0. \tag{56}$$

  Because $\mathcal{W}_m$ is initially set to be equal to $\mathscr{V}_m$ and then is updated by Equation (28), which has full column rank, taking a left inverse for the Moore-Penrose inverse of $\mathcal{W}_m$ makes $\mathcal{W}_m^{\dagger}\mathcal{W}_m = I$. Therefore, the second formula of (56) equivalently becomes

$$(A\widehat{\mathscr{Z}_m})^H\,(A\widehat{\mathscr{Z}_m}g_i - \theta_i\,\mathcal{W}_m g_i) = 0. \tag{57}$$

  Using Equation (26) leads to

$$\left(\widehat{\mathscr{V}}_{m+1}\underline{\mathscr{F}}_m\right)^H\,\left(\widehat{\mathscr{V}}_{m+1}\underline{\mathscr{F}}_m g_i - \theta_i\,\mathcal{W}_m g_i\right) = 0. \tag{58}$$

  Because $\widehat{\mathscr{V}}_{m+1} = [C_k, \mathscr{V}_m, [P_{m-1}, \widetilde{W}_m]]$ generated at the end of each cycle is orthonormal, Equation (58) becomes

$$\underline{\mathscr{F}}_m^H\underline{\mathscr{F}}_m g_i - \theta_i\underline{\mathscr{F}}_m^H\widehat{\mathscr{V}}_{m+1}^H\mathcal{W}_m g_i = 0,$$

  which is the same as formulation (27).

- Let Q and R be the factors of the reduced QR-factorization of $\underline{\mathscr{F}}_m G_k$ and multiply by G_k on the both sides of Equation (26). It leads to $A\widehat{\mathscr{Z}_m}G_k = \widehat{\mathscr{V}}_{m+1}\underline{\mathscr{F}}_m G_k = \widehat{\mathscr{V}}_{m+1}QR$, that is equivalent to $A\widehat{\mathscr{Z}_m}G_k R^{-1} = \widehat{\mathscr{V}}_{m+1}\underline{\mathscr{F}}_m G_k R^{-1} = \widehat{\mathscr{V}}_{m+1}Q$ that concludes the proof as $\widehat{\mathscr{V}}_{m+1}Q$ is the product of two matrices with orthonormal columns so are its columns.

- The same process for proving Corollary 1.

□

C IB-BFGMRES-DR: Block flexible GMRES with inexact breakdowns and deflated restarting

C.1 Block flexible Arnoldi with inexact breakdowns

Starting from an orthonormal block vector $\mathbb{V}_1$ obtained from the reduced QR-factorization of the initial residual block (denoted as R_0 in this Section)[1] $R_0 = B - AX_0 = \mathbb{V}_1\Lambda_1$, Algorithm 3 describes details about the block flexible Arnoldi process used to construct a pair of orthonormal basis. In the no exact breakdown situation, i.e., $p_{j+1} = p_j = \ldots = p_1 = p$, the whole columns of $\mathbb{W}_j$ in step 10 of Algorithm 3 have been used to enlarge the search space, and then the block Arnoldi relation at the jth iteration is obtained as

$$A\mathscr{Z}_j = \mathscr{V}_j\mathscr{H}_j + [0_{n\times n_{j-1}}, \quad \mathbb{W}_j] = \mathscr{V}_{j+1}\underline{\mathscr{H}}_j, \tag{59}$$

in which $\mathscr{Z}_j = [\mathscr{M}_1(\mathbb{V}_1), ..., \mathscr{M}_m(\mathbb{V}_j)]$, $\mathscr{V}_j = [\mathbb{V}_1, ..., \mathbb{V}_j] \in \mathbb{C}^{n\times n_j}$ ($n_j = j \times p$) contains orthonormal columns and $\underline{\mathscr{H}}_j = \begin{bmatrix} \mathscr{H}_j \\ 0_{\ldots 0}\ H_{j+1,j} \end{bmatrix} \in \mathbb{C}^{n_{j+1}\times n_j}$ composed by square matrices $H_{j+1,j} \in \mathbb{C}^{p_j\times p_j}$ ($p_j = p$) is a block upper Hessenberg matrix. The minimum residual norm solution in the affine space $X_0 + \mathrm{Range}(\mathscr{Z}_j)$ can be written as $X_j = X_0 + \mathscr{Z}_j Y_j$ where

$$Y_j = \underset{Y\in\mathbb{C}^{n_j\times p}}{\mathrm{argmin}} \|\tilde{\Lambda}_j - \underline{\mathscr{H}}_j Y\|_F$$

and $\tilde{\Lambda}_j = \mathscr{V}_{j+1}^H R_0 = (\Lambda_1, 0_{n_j\times p})^T$, the columns of $\tilde{\Lambda}_j$ are the components of the individual initial residual in the residual space $\mathscr{V}_{j+1}$.

Algorithm 3 *BLOCK FLEXIBLE ARNOLDI PROCEDURE WITH BLOCKWISE MODIFIED GRAM-SCHMIDT ORTHOGONALIZATION:*

1: Given a nonsingular coefficient matrix $A \in \mathbb{C}^{n\times n}$, choose a unitary matrix V_1 of size $n \times p$
2: **for** $j = 1, 2, \ldots, m$ **do**
3: Choose a (possibly nonlinear) preconditioning operator $\mathscr{M}_j$
4: $Z_j = \mathscr{M}_j(\mathbb{V}_j)$
5: Compute $\mathbb{W}_j = AZ_j$
6: **for** $i = 1, 2, \ldots, j$ **do**
7: $H_{i,j} = \mathbb{V}_i^H \mathbb{W}_j$
8: $\mathbb{W}_j = \mathbb{W}_j - \mathbb{V}_i H_{i,j}$
9: **end for**
10: $\mathbb{W}_j = \mathbb{V}_{j+1} H_{j+1,j}$ (reduced QR-factorization)
11: **end for**

When an inexact breakdown occurs up to iteration j in Algorithm 3, the dimension of the approximation space $\mathrm{Range}(\mathscr{Z}_j)$ generated at the jth iteration is no longer equal to $j \times p$ but equal to $n_j = \sum_{i=1}^{j} p_i$ with $n_j < j \times p$. According to the inexact breakdown detecting mechanism in IB-BGMRES [19], the block flexible Arnoldi with inexact breakdowns [2] and Equation (9) developed by Robbé and Sadkane [19],

[1] Out of simplicity, the initial residual block in here is assumed to be of full column rank, while such assumption could be removed by introducing inexact breakdown detection in initial residual block as the contents described in Section 4.1.

[2] The block flexible Arnoldi with inexact breakdowns is obtained by changing the step 11 of Algorithm 2 into
11: Orthogonalize $A\mathscr{M}_j(\mathbb{V}_j)$ against previous block orthonormal vector $\mathscr{V}_j = [\mathbb{V}_1, \ldots, \mathbb{V}_j]$ as

$$\mathscr{L}_{1,1:j} = \mathscr{V}_j^H(A\mathscr{M}_j(\mathbb{V}_j)),\ W_j = A\mathscr{M}_j(\mathbb{V}_j) - \mathscr{V}_j\mathscr{L}_{1,1:j},\ \text{where } \mathscr{L}_{1,1:j} \text{ is a block column matrix.}$$

the Equation (59) could be extended into

$$A\mathscr{Z}_j = \mathscr{V}_j\mathscr{H}_j + [\mathcal{Q}_{j-1}, \quad \mathbb{W}_j], \tag{60}$$

where $\mathcal{Q}_{j-1} = [Q_1, \ldots, Q_{j-1}] \in \mathbb{C}^{n\times n_{j-1}}$ is rank deficient and accounts for all the abandoned directions.

In order to characterize a minimum norm solution in the space spanned by $\mathscr{Z}_j$ using Equation (60) we need to form an orthonormal basis of the space spanned by $[\mathscr{V}_j, \mathcal{Q}_{j-1}, \mathbb{W}_j]$. This is performed by first orthogonalizing $\mathcal{Q}_{j-1}$ against $\mathscr{V}_j$, that is $\widetilde{\mathcal{Q}}_{j-1} = (I - \mathscr{V}_j\mathscr{V}_j^H)\mathcal{Q}_{j-1}$. Because $\mathcal{Q}_{j-1}$ is of low rank so is $\widetilde{\mathcal{Q}}_{j-1}$ that can be written as formula (11). Next $\mathbb{W}_j$, that is already orthogonal to $\mathscr{V}_j$, is made to be orthogonal to P_{j-1} with $\mathbb{W}_j - P_{j-1}E_j$ where $E_j = P_{j-1}^H\mathbb{W}_j$; then one computes $\widetilde{W}_jD_j$ the reduced QR-factorization of $\mathbb{W}_j - P_{j-1}E_j$. Eventually, the columns of the matrix $[\mathscr{V}_j, P_{j-1}, \widetilde{W}_j]$ form an orthonormal basis of the space spanned by $[\mathscr{V}_j, \mathcal{Q}_{j-1}, \mathbb{W}_j]$.

With this new basis Equation (60) writes

$$A\mathscr{Z}_j \quad = \quad \left[\mathscr{V}_j, [P_{j-1}, \widetilde{W}_j]\right] \underline{\tilde{\mathscr{F}}}_j, \tag{61}$$

where $\underline{\tilde{\mathscr{F}}}_j = \begin{bmatrix} \mathscr{L}_j \\ \widehat{\mathbb{H}}_j \end{bmatrix} \in \mathbb{C}^{(n_j+p)\times n_j}$ with $\widehat{\mathbb{H}}_j = \begin{bmatrix} \mathbb{G}_{j-1} & E_j \\ 0 & D_j \end{bmatrix} \in \mathbb{C}^{p\times n_j}$ (here the notation $\mathbb{H}_j$ with the wide-hat form is used for distinguishing from that already used in IB-BGCRO-DR case as appeared in Equation (14) and (38)) and $\mathscr{L}_j \in \mathbb{C}^{n_j\times n_j}$ owns the same details as described in formula (12), which is no longer a block upper Hessenberg as shown in the right-hand sides of Equation (59) as soon as inexact breakdown occurs, i.e., $\exists \ell \; Q_\ell \neq 0$.

The numerical mechanism to select V_{j+1} out of $\left[P_{j-1}, \widetilde{W}_j\right]$ follows the same ideas as discussed in [1, 19] within the context of block GMRES. The governing idea consists in building the orthonormal basis for the directions that contribute the most to the individual residual norms and make them larger than the target threshold τ. Based on the SVD of the coordinate vector of the scaled least squares residual $(\tilde{\Lambda}_j - \underline{\tilde{\mathscr{F}}}_j Y_j)D_\varepsilon = \mathbb{U}_{1,L}\Sigma_1\mathbb{V}_{1,R}^H + \mathbb{U}_{2,L}\Sigma_2\mathbb{V}_{2,R}^H$ where D_ε is a diagonal matrix used to select the space expansion described in the Section 3, Σ_1 contains the singular values larger than the prescribed IB-threshold τ, they decompose $\mathbb{U}_{1,L} = \begin{pmatrix} \mathbb{U}_1^{(1)} \\ \mathbb{U}_1^{(2)} \end{pmatrix}$ in accordance with $\left[\mathscr{V}_j, [P_{j-1}, \widetilde{W}_j]\right]$, that is $\mathbb{U}_1^{(1)} \in \mathbb{C}^{n_j\times p}$ and $\mathbb{U}_1^{(2)} \in \mathbb{C}^{p\times p}$. Because, the objective is to construct orthonormal basis we consider $[\mathbb{W}_1, \mathbb{W}_2]$ unitary so that $\mathrm{Range}(\mathbb{W}_1) = \mathrm{Range}(\mathbb{U}_1^{(2)})$. The new set of orthonormal vectors selected to expand the search space as formula (16), which contributes the most to the residual. We do not give the detailed calculation and refer to [19] for a complete description, but only state that via this decomposition the main terms that appear in Equation (61) can be computed incrementally by an alternative formulation:

$$A\mathscr{Z}_j \quad = \quad \mathscr{V}_{j+1}\underline{\mathscr{L}}_j + \widetilde{\mathcal{Q}}_j, \tag{62}$$

with $\underline{\mathscr{L}}_j = \begin{bmatrix} \mathscr{L}_j \\ V_{j+1}\mathcal{Q}_{j-1} \; \mathrm{H}_{j+1,j} \end{bmatrix}$, where $\mathscr{L}_j = \begin{bmatrix} & H_{1,j} \\ \underline{\mathscr{L}}_{j-1} & \vdots \\ & H_{j,j} \end{bmatrix}$, the last block row of $\underline{\mathscr{L}}_j$ at next iteration $(j+1)$ is given by $\underline{\mathscr{L}}_{j+1,:} = \mathbb{W}_1^H\widehat{\mathbb{H}}_j$. The last block column of $\mathscr{L}_{j+1}$ results from the block flexible Arnoldi orthogonalization. The new compressed form of the abandoned direction $\widetilde{\mathcal{Q}}_j$ is given by the new orthonomal set of vectors

$$P_j = \left[P_{j-1}, \widetilde{W}_j\right] \mathbb{W}_2, \tag{63}$$

and the complementary part of V_{j+1} and their components in the space spanned by P_j are $\mathbb{G}_j = \mathbb{W}_2^H\widehat{\mathbb{H}}_j$.

Consequently, in one cycle of IB-BFGMRES-DR, once the maximum size of the space has been reached, we have

$$\begin{aligned} A\mathscr{Z}_m &= \left[\mathscr{V}_m, [P_{m-1}, \widetilde{W}_m]\right] \underline{\tilde{\mathscr{F}}}_m, && (64)\\ A\mathscr{Z}_m &= \mathscr{V}_{m+1}\underline{\mathscr{L}}_m + \widetilde{\mathcal{Q}}_m, && (65)\\ X_m &= X_0 + \mathscr{Z}_m Y_m, && (66)\\ R_m &= \left[\mathscr{V}_m, [P_{m-1}, \widetilde{W}_m]\right] \left(\tilde{\Lambda}_m - \underline{\tilde{\mathscr{F}}}_m Y_m\right), && (67)\\ Y_m &= \underset{Y\in\mathbb{C}^{n_m\times p}}{\operatorname{argmin}} \left\|\tilde{\Lambda}_m - \underline{\tilde{\mathscr{F}}}_m Y\right\|_F, \tilde{\Lambda}_m = [\Lambda_1^T, 0_{p\times n_m}]^T. \end{aligned}$$

C.2 Harmonic-Ritz vectors and residuals

We first illustrate how to compute the harmonic-Ritz vectors used for deflation as described in Proposition 7 and then discuss the relation between the linear system residuals and the residuals of harmonic-Ritz vectors at the restart of IB-BFGMRES-DR.

Proposition 7. *At the end of a cycle of IB-BFGMRES-DR, the updating of deflated restarting used in next cycle relies on the computation of k harmonic-Ritz vectors $Y_k = \mathscr{V}_m G_k$ of $A\mathscr{Z}_m\mathscr{V}_m^H$ with respect to* $\mathrm{Range}(\mathscr{V}_m)$*, where each harmonic-Ritz pair $(\theta_j, \mathscr{V}_m g_j)$ computed at the end of cycle satisfies*

$$(\mathscr{L}_m + \mathscr{L}_m^{-H}\,\widehat{\mathbb{H}}_m^H\widehat{\mathbb{H}}_m)g_j = \theta_j\, g_j \quad \textit{for } 1 \le j \le k, \tag{68}$$

where $\mathscr{L}_m \in \mathbb{C}^{n_m\times n_m}$ and $\widehat{\mathbb{H}}_m \in \mathbb{C}^{p\times n_m}$.

Proof. According to Definition 1, each harmonic-Ritz pair $(\theta_j, \mathscr{V}_m g_j)$ satisfies

$$\forall w \in \mathrm{Range}(A\mathscr{Z}_m\mathscr{V}_m^H\mathscr{V}_m) \quad w^H\,(A\mathscr{Z}_m\mathscr{V}_m^H\mathscr{V}_m g_j - \theta_j\,\mathscr{V}_m g_j) = 0,$$

which is equivalent to

$$(A\mathscr{Z}_m)^H\,(A\mathscr{Z}_m g_j - \theta_j\,\mathscr{V}_m g_j) = 0,$$

by the orthonormality of $\mathscr{V}_m$. Substituting Equation (64) into the above one yields

$$(\left[\mathscr{V}_m, [P_{m-1}, \widetilde{W}_m]\right] \underline{\tilde{\mathscr{F}}}_m)^H\,(\left[\mathscr{V}_j, [P_{m-1}, \widetilde{W}_m]\right] \underline{\tilde{\mathscr{F}}}_m\, g_j - \theta_j\,\mathscr{V}_m\, g_j) = 0. \tag{69}$$

Because of the structure of $\underline{\tilde{\mathscr{F}}}_m$ and the orthonormality of $[\mathscr{V}_m, P_{m-1}, \widetilde{W}_m]$, Equation (69) becomes

$$(\mathscr{L}_m^H\,\mathscr{L}_m + \widehat{\mathbb{H}}_m^H\widehat{\mathbb{H}}_m)g_j = \theta_j\,\mathscr{L}_m^H g_j, \tag{70}$$

which completes the proof since $\mathscr{L}_m$ is assumed to be nonsingular. □

Assume $R_m^{LS} = \left(\tilde{\Lambda}_m - \underline{\tilde{\mathscr{F}}}_m Y_m\right) \in \mathbb{C}^{(n_m+p)\times p}$, the residual of linear system presented in Equation (67) could be simplified as

$$R_m = \left[\mathscr{V}_m, [P_{m-1}, \widetilde{W}_m]\right] R_m^{LS} \in \mathbb{C}^{n\times p}. \tag{71}$$

Denote the corresponding residual of harmonic-Ritz vectors as $R_m^{(HR)}$ similarly, which owns form as

$$R_m^{(HR)} = A\mathscr{Z}_m G_k - \mathscr{V}_m G_k\,\mathrm{diag}(\theta_1, \ldots, \theta_k) \in \mathbb{C}^{n\times k}. \tag{72}$$

Given that both R_m and $R_m^{(HR)}$ are resided in the subspace $\mathrm{Range}(\left[\mathscr{V}_m, [P_{m-1}, \widetilde{W}_m]\right]) \in \mathbb{C}^{n\times(n_m+p)}$ and are orthogonal to the same subspace $\mathrm{Range}(A\mathscr{Z}_m) \in \mathbb{C}^{n\times n_m}$. Therefore, the residuals of linear system R_m and the residuals of harmonic-Ritz vectors $R_m^{(HR)}$ are in the same p-dimensional space denoted as $\mathrm{Range}(A\mathscr{Z}_m)^{\perp} \cap \mathrm{Range}(\left[\mathscr{V}_m, [P_{m-1}, \widetilde{W}_m]\right])$, which means there exists a matrix $\beta_{p\times k} \in \mathbb{C}^{p\times k}$ such that $R_m^{(HR)} = R_m\beta_{p\times k}$. According to Equation (71) and (72), such collinear relationship between the linear system residuals and residuals of harmonic-Ritz vectors could be further described as the following formula

$$A\mathscr{Z}_m G_k = \left[\mathscr{V}_m, [P_{m-1}, \widetilde{W}_m]\right] \underline{G} \begin{bmatrix} diag(\theta_1, \cdots, \theta_k) \\ \beta_{p\times k} \end{bmatrix}, \tag{73}$$

where $G_k = [g_1, \ldots, g_k] \in \mathbb{C}^{n_m\times k}$, $\underline{G} = \begin{bmatrix} G_k & R_m^{LS} \\ 0_{p\times k} & \end{bmatrix} \in \mathbb{C}^{(n_m+p)\times(k+p)}$, $\beta_{p\times k} = (\beta_1, \cdots, \beta_k) \in \mathbb{C}^{p\times k}$ and $\beta_i \in \mathbb{C}^p$ $(1 \le i \le k)$. Based on Equation (61) and the orthonormality of $\left[\mathscr{V}_m, [P_{m-1}, \widetilde{W}_m]\right]$, Equation (73) can be also expressed as

$$\underline{\tilde{\mathscr{F}}}_m G_k = \underline{G} \begin{bmatrix} diag(\theta_1, \cdots, \theta_k) \\ \beta_{p\times k} \end{bmatrix}, \tag{74}$$

which is the block form of Equation (3.4) shown in [1, Lemma3.3].

C.3 Flexible block GMRES with inexact breakdowns at restart

In this section, the forthcoming Theorem 2 will be presented to illustrate that the flexible Arnoldi relation with inexact breakdowns described in Equation (61) and (62) (or in Equation (64) and (65)) still hold at restart of IB-BFGMRES-DR. Firstly, let us denote $\underline{G} = Q_{\underline{G}}R_{\underline{G}}$ the reduced QR-factorization of $\underline{G}$ shown in Equation (74) and the reduced factors could be partitioned as

$$Q_{\underline{G}} = \begin{bmatrix} \Gamma_1 & \Gamma_2 \\ 0_{p\times k} & \end{bmatrix} \in \mathbb{C}^{(n_m+p)\times(k+p)}, \tag{75}$$

$$R_{\underline{G}} = \begin{bmatrix} \Theta_1 & \Theta_2 \\ 0_{p\times k} & \end{bmatrix} \in \mathbb{C}^{(k+p)\times(k+p)}, \tag{76}$$

with $\Gamma_1 = Q_{\underline{G}}(1:n_m, 1:k)$, $\Gamma_2 = Q_{\underline{G}}(:, k+1:k+p)$, $\Theta_1 = R_{\underline{G}}(1:k, 1:k)$, $\Theta_2 = R_{\underline{G}}(:, k+1:k+p)$ and

$$G_k = \Gamma_1\Theta_1, \tag{77}$$

$$R_m^{LS} = Q_{\underline{G}}\Theta_2. \tag{78}$$

Theorem 2. *At each restart of IB-BFGMRES-DR, the initial block-flexible-Arnoldi-like relation* (61) *and* (62) *still hold in exact arithmetic as*

$$A\mathscr{Z}_1^{new} = \left[\mathscr{V}_1^{new}, [P_0, \widetilde{W}_1]^{new}\right] \underline{\tilde{\mathscr{F}}}_1^{new}, \tag{79}$$

$$A\mathscr{Z}_1^{new} = \mathscr{V}_2^{new}\underline{\mathscr{L}}_1^{new} + \widetilde{\mathcal{Q}}_1^{new}, \tag{80}$$

$$R_0^{new} = R_m = \left[\mathscr{V}_1^{new}, [P_0, \widetilde{W}_1]^{new}\right] \tilde{\Lambda}_1^{new} \text{ and } \tilde{\Lambda}_1^{new} = \Theta_2, \tag{81}$$

with

$$\begin{aligned}
\mathscr{Z}_1^{new} &= \mathscr{Z}_m\Gamma_1,\ \left[\mathscr{V}_1^{new}, [P_0, \widetilde{W}_1]^{new}\right] = \left[\mathscr{V}_m, [P_{m-1}, \widetilde{W}_m]\right] Q_{\underline{G}},\\
\mathscr{V}_1^{new} &= \mathscr{V}_m\Gamma_1,\ [P_0, \widetilde{W}_1]^{new} = \left[\mathscr{V}_m, [P_{m-1}, \widetilde{W}_m]\right] \Gamma_2,\\
\underline{\tilde{\mathscr{F}}}_1^{new} &= \begin{bmatrix} \mathscr{L}_1^{\mathrm{new}} \\ \widehat{\mathbb{H}}_1^{new} \end{bmatrix} \textit{ and } \mathscr{L}_1^{new} = \Gamma_1^H \mathscr{L}_m\Gamma_1,\ \widehat{\mathbb{H}}_1^{new} = \Gamma_2^H \underline{\tilde{\mathscr{F}}}_m\Gamma_1,\\
\mathbb{V}_2^{new} &= [P_0, \widetilde{W}_1]^{new}\mathbb{W}_1,\ \mathscr{V}_2^{new} = [\mathscr{V}_1^{new}, \mathbb{V}_2^{new}],\\
\mathscr{L}_{2,:}^{new} &= \mathbb{W}_1^H \widehat{\mathbb{H}}_1^{new},\ \underline{\mathscr{L}}_1^{new} = \begin{bmatrix} \mathscr{L}_1^{new} \\ \mathscr{L}_{2,:}^{new} \end{bmatrix},\\
P_1^{new} &= [P_0, \widetilde{W}_1]^{new}\mathbb{W}_2,\ \mathbb{G}_1^{new} = \mathbb{W}_2^H \widehat{\mathbb{H}}_1^{new},\ \widetilde{\mathcal{Q}}_1^{new} = P_1^{new}\mathbb{G}_1^{new},
\end{aligned}$$

where $\mathbb{W}_1$ *and* $\mathbb{W}_2$ *satisfy*

$$\mathrm{Range}(\mathbb{W}_1) = \mathrm{Range}(\mathbb{U}_1^{new(2)}) \textit{ with } \mathbb{U}_{1,L}^{new} = \begin{bmatrix} \mathbb{U}_1^{new(1)} \\ \mathbb{U}_1^{new(2)} \end{bmatrix} \textit{ and } [\mathbb{W}_1\ \mathbb{W}_2] \textit{ is unitary}$$

with

$$(\tilde{\Lambda}_1^{new} - \underline{\tilde{\mathscr{F}}}_1^{new} Y_1^{new}) D_\epsilon = \mathbb{U}_{1,L}^{new}\Sigma_1^{new}\mathbb{V}_{1,R}^{new\,H} + \mathbb{U}_{2,L}^{new}\Sigma_2^{new}\mathbb{V}_{2,R}^{new\,H},$$

where $\sigma_{min}(\Sigma_1^{new}) \geq 1 \geq \sigma_{max}(\Sigma_2^{new})$, *the SVD to detect inexact breakdown in the restarting scaled least squares residual block where*

$$Y_1^{new} = \underset{Y\in\mathbb{C}^{n_1\times p}}{\mathrm{argmin}} \left\| \tilde{\Lambda}_1^{new} - \underline{\tilde{\mathscr{F}}}_1^{new} Y \right\|_F.$$

Proof. Starting from the relationship between residual and harmonic-Ritz vectors as shown in Equation (73), let's substitute $\underline{G}$ by these reduced factors $Q_{\underline{G}}$ in Equation (75) and $R_{\underline{G}}$ in (76) obtained by its reduced QR-factorization and change G_k by relation (77), then we have

$$A\mathscr{Z}_m\Gamma_1 = \left[\mathscr{V}_m, [P_{m-1}, \widetilde{W}_m]\right] Q_{\underline{G}} R_{\underline{G}} \begin{bmatrix} diag(\theta_1, \cdots, \theta_k) \\ \beta_{p\times k} \end{bmatrix} \Theta_1^{-1}$$

by the nonsingularity of Θ_1, which could be rewritten as

$$A\mathscr{Z}_m\Gamma_1 = \left[\mathscr{V}_m\Gamma_1, [\mathscr{V}_m, [P_{m-1}, \widetilde{W}_m]]\Gamma_2\right] R_{\underline{G}} \begin{bmatrix} diag(\theta_1, \cdots, \theta_k) \\ \beta_{p\times k} \end{bmatrix} \Theta_1^{-1} \tag{82}$$

because of the partition of $Q_{\underline{G}}$ shown in Equation (75). Then, repeating the same processes described above, the corresponding formula (74) could also be reformed as

$$\underline{\tilde{\mathscr{F}}}_m\Gamma_1 = Q_{\underline{G}} R_{\underline{G}} \begin{bmatrix} diag(\theta_1, \cdots, \theta_k) \\ \beta_{p\times k} \end{bmatrix} \Theta_1^{-1},$$

from which, we have

$$R_{\underline{G}} \begin{bmatrix} diag(\theta_1, \cdots, \theta_k) \\ \beta_{p\times k} \end{bmatrix} \Theta_1^{-1} = Q_{\underline{G}}^H \underline{\tilde{\mathscr{F}}}_m\Gamma_1.$$

According to the structure of $Q_{\underline{G}}$ and $\mathscr{F}_m$ as shown in Equation (75) and (61), we obtain

$$R_{\underline{G}} \begin{bmatrix} diag(\theta_1, \cdots, \theta_k) \\ \beta_{p\times k} \end{bmatrix} \Theta_1^{-1} = \begin{bmatrix} \Gamma_1^{\mathrm{H}}\mathscr{L}_{\mathrm{m}}\Gamma_1 \\ \Gamma_2^H \underline{\tilde{\mathscr{F}}}_m\Gamma_1 \end{bmatrix}. \tag{83}$$

If we denote

$$\begin{aligned}\mathscr{Z}_1^{new} &= \mathscr{Z}_m\Gamma_1,\ \mathscr{V}_1^{new} = \mathscr{V}_m\Gamma_1,\ [P_0,\widetilde{W}_1]^{new} = \left[\mathscr{V}_m,[P_{m-1},\widetilde{W}_m]\right]\Gamma_2,\\ \mathscr{L}_1^{new} &= \Gamma_1^H\mathscr{L}_m\Gamma_1,\ \widehat{\mathbb{H}}_1^{new} = \Gamma_2^H\underline{\tilde{\mathscr{F}}}_m\Gamma_1, \underline{\tilde{\mathscr{F}}}_1^{new} = \begin{bmatrix}\mathscr{L}_1^{\rm new}\\ \widehat{\mathbb{H}}_1^{new}\end{bmatrix},\end{aligned}$$

and substitute Equation (83) into (82), then Equation (79) is proven.

Next, show that equality (80) holds. Given $[\mathbb{W}_1\ \mathbb{W}_2]$ is unitary, we have

$$[P_0,\widetilde{W}_1]^{new} = [P_0,\widetilde{W}_1]^{new}[\mathbb{W}_1\mathbb{W}_1^H + \mathbb{W}_2\mathbb{W}_2^H],$$

and substituting this into Equation (79) gives

$$\begin{aligned}A\mathscr{Z}_1^{new} &= \left[\mathscr{V}_1^{new},[P_0,\widetilde{W}_1]^{new}[\mathbb{W}_1\mathbb{W}_1^H+\mathbb{W}_2\mathbb{W}_2^H]\right]\begin{bmatrix}\mathscr{L}_1^{\rm new}\\ \widehat{\mathbb{H}}_1^{new}\end{bmatrix},\\ &= \mathscr{V}_1^{new}\mathscr{L}_1^{new} + [P_0,\widetilde{W}_1]^{new}[\mathbb{W}_1\mathbb{W}_1^H+\mathbb{W}_2\mathbb{W}_2^H]\widehat{\mathbb{H}}_1^{new},\\ &= \mathscr{V}_1^{new}\mathscr{L}_1^{new} + [P_0,\widetilde{W}_1]^{new}\mathbb{W}_1\mathbb{W}_1^H\widehat{\mathbb{H}}_1^{new} + [P_0,\widetilde{W}_1]^{new}\mathbb{W}_2\mathbb{W}_2^H\widehat{\mathbb{H}}_1^{new},\\ &= \mathscr{V}_1^{new}\mathscr{L}_1^{new} + \mathbb{V}_2^{new}\mathscr{L}_{2,:}^{new} + P_1^{new}\mathbb{G}_1^{new},\\ &= [\mathscr{V}_1^{new}\,V_2^{new}]\begin{bmatrix}\mathscr{L}_1^{new}\\ \mathscr{L}_{2,:}^{new}\end{bmatrix} + P_1^{new}\mathbb{G}_1^{new},\end{aligned}$$

which is relation (80).

From Equation (71) and (78), at restart we have

$$\begin{aligned}R_0^{new} &= R_m = \left[\mathscr{V}_m,[P_{m-1},\widetilde{W}_m]\right]R_m^{LS}\\ &= \left[\mathscr{V}_m,[P_{m-1},\widetilde{W}_m]\right]Q_{\underline{G}}\Theta_2 = \left[\mathscr{V}_1^{new},[P_0,\widetilde{W}_1]^{new}\right]\tilde{\Lambda}_1^{new}.\end{aligned}$$

This completes the proof. □

D Proof of Proposition 4

Proof. From Equation (36), (37) and (39), the initial residual block R_1 with inexact breakdown detection at restart could be described as

$$\begin{aligned} R_1 &= [C_k, \mathbb{V}_1, P_0, \widetilde{W}_1][C_k, \mathbb{V}_1, P_0, \widetilde{W}_1]^H R_1 = [C_k, \mathbb{V}_1, P_0, \widetilde{W}_1][C_k, \mathbb{V}_1, P_0, \widetilde{W}_1]^H [\mathbb{V}_1^{new}, P_0^{new}]\hat{\Lambda}_1 \\ &= [C_k, \mathbb{V}_1, P_0, \widetilde{W}_1] \left([C_k, \mathbb{V}_1, P_0, \widetilde{W}_1]^H C_k R_{12} + [C_k, \mathbb{V}_1, P_0, \widetilde{W}_1]^H [\mathbb{V}_1, P_0] R_{22} \right) \hat{\Lambda}_1 \\ &= [C_k, \mathbb{V}_1, P_0, \widetilde{W}_1]\Lambda_1 \text{ with } \Lambda_1 = \begin{bmatrix} R_{12} \\ 0_{(p_1+p)\times p} \end{bmatrix} \hat{\Lambda}_1 + \begin{bmatrix} 0_{k\times p_1} & 0_{k\times q_1} \\ I_{p_1} & 0_{p_1\times q_1} \\ 0_{q_1\times p_1} & I_{q_1} \\ 0_{p_1\times p_1} & 0_{p_1\times q_1} \end{bmatrix} R_{22}\hat{\Lambda}_1, \end{aligned}$$

by $[\mathbb{V}_1^{new}, P_0^{new}] = C_k R_{12} + [\mathbb{V}_1, P_0] R_{22}$ obtained from Equation (37). That can also be written as

$$\Lambda_1 = \begin{bmatrix} R_{12} \\ 0_{(p_1+p)\times p} \end{bmatrix} \hat{\Lambda}_1 + \begin{bmatrix} 0_{k\times p_1} & 0_{k\times q_1} \\ I_{p_1} & \Phi_1 \\ 0_{q_1\times p_1} & \\ 0_{p_1\times p_1} & 0_{p_1\times q_1} \end{bmatrix} R_{22}\hat{\Lambda}_1,$$

where $\Phi_1 = \begin{bmatrix} 0_{p_1\times q_1} \\ I_{q_1} \end{bmatrix} \in \mathbb{C}^{p\times q_1}$ and $q_1 + p_1 = p$.

The right-hand sides of the least-squares problem at iteration $(j+1)$ for $j = 1, 2, \cdots$, are defined by

$$
\begin{aligned}
\Lambda_{j+1} &= [C_k, \mathscr{V}_{j+1}, [P_j, \widetilde{W}_{j+1}]]^H R_1 = [C_k, \mathscr{V}_j, V_{j+1}, [P_j, \widetilde{W}_{j+1}]]^H R_1 \\
&= \left[C_k, \mathscr{V}_j, [P_{j-1}, \widetilde{W}_j]\mathbb{W}_1, [P_{j-1}, \widetilde{W}_j]\mathbb{W}_2, \widetilde{W}_{j+1}\right]^H R_1 = \left[C_k, \mathscr{V}_j, [P_{j-1}, \widetilde{W}_j][\mathbb{W}_1, \mathbb{W}_2], \widetilde{W}_{j+1}\right]^H [\mathbb{V}_1^{new}, P_0^{new}]\hat{\Lambda}_1 \\
&= \left(\left[C_k, \mathscr{V}_j, [P_{j-1}, \widetilde{W}_j][\mathbb{W}_1, \mathbb{W}_2], \widetilde{W}_{j+1}\right]^H C_k R_{12} + \left[C_k, \mathscr{V}_j, [P_{j-1}, \widetilde{W}_j][\mathbb{W}_1, \mathbb{W}_2], \widetilde{W}_{j+1}\right]^H [\mathbb{V}_1, P_0] R_{22}\right)\hat{\Lambda}_1 \\
&= \begin{bmatrix} R_{12} \\ 0_{(n_j+p+p_{j+1})\times p} \end{bmatrix}\hat{\Lambda}_1 + \begin{bmatrix} C_k^H\mathbb{V}_1 & C_k^H P_0 \\ \mathscr{V}_j^H\mathbb{V}_1 & \mathscr{V}_j^H P_0 \\ [V_{j+1}, P_j]^H\mathbb{V}_1 & [\mathbb{W}_1, \mathbb{W}_2]^H\left[P_{j-1}, \widetilde{W}_j\right]^H P_0 \\ \widetilde{W}_{j+1}^H\mathbb{V}_1 & \widetilde{W}_{j+1}^H P_0 \end{bmatrix} R_{22}\hat{\Lambda}_1 \\
&= \begin{bmatrix} R_{12} \\ 0_{(n_j+p+p_{j+1})\times p} \end{bmatrix}\hat{\Lambda}_1 + \begin{bmatrix} 0_{k\times p_1} & 0_{k\times q_1} \\ \begin{bmatrix} I_{p_1} \\ 0_{(n_j-p_1)\times p_1} \end{bmatrix} & \Phi_j(1:n_j,:) \\ 0_{p\times p_1} & [\mathbb{W}_1, \mathbb{W}_2]^H \begin{bmatrix} P_{j-1}^H \\ \widetilde{W}_j^H \end{bmatrix} P_0 \\ 0_{p_{j+1}\times p_1} & 0_{p_{j+1}\times q_1} \end{bmatrix} R_{22}\hat{\Lambda}_1 \\
&= \begin{bmatrix} R_{12} \\ 0_{(n_j+p+p_{j+1})\times p} \end{bmatrix}\hat{\Lambda}_1 + \begin{bmatrix} 0_{k\times p_1} & 0_{k\times q_1} \\ \begin{bmatrix} I_{p_1} \\ 0_{(n_j-p_1)\times p_1} \end{bmatrix} & \Phi_j(1:n_j,:) \\ 0_{p\times p_1} & [\mathbb{W}_1, \mathbb{W}_2]^H \begin{bmatrix} \Phi_j(n_j+1:n_j+q_j,:) \\ 0_{p_j\times q_1} \end{bmatrix} \\ 0_{p_{j+1}\times p_1} & 0_{p_{j+1}\times q_1} \end{bmatrix} R_{22}\hat{\Lambda}_1 \\
&= \begin{bmatrix} R_{12} \\ 0_{(n_j+p+p_{j+1})\times p} \end{bmatrix}\hat{\Lambda}_1 + \begin{bmatrix} 0_{k\times p_1} & 0_{k\times q_1} \\ \begin{bmatrix} I_{p_1} \\ 0_{(n_j+p-p_1)\times p_1} \end{bmatrix} & \Phi_{j+1} \\ 0_{p_{j+1}\times p_1} & 0_{p_{j+1}\times q_1} \end{bmatrix} R_{22}\hat{\Lambda}_1
\end{aligned}
$$

where $\Phi_{j+1} \in \mathbb{C}^{(n_j+p)\times q_1}$ for $j = 1, 2, \cdots$. □

E The SVD decomposition of the least squares residual and the solution of the least-squares problem

The inexact breakdown (IB) mechanism allows to extract from the residual spaces new directions to expand the search space at the next iteration of the block method. The selection consists in extracting the directions that contribute the most to the scaled residual block and is based on the SVD of the scaled least squares residual. In this section, we detail how the solution of the least-squares problem (13) enables to compute easily and cheaply the SVD of the associated scaled (least squares) residual block. The least-squares problem

$$Y_j = \underset{Y\in\mathbb{C}^{(k+n_j)\times p}}{\operatorname{argmin}} \left\|\Lambda_j - \underline{\mathscr{F}}_j Y\right\|_F, \text{ with } \underline{\mathscr{F}}_j \in \mathbb{C}^{(k+n_j+p)\times(k+n_j)} \tag{84}$$

is solved by using a full QR-factorization of $\underline{\mathscr{F}}_j = Q_j^{LS} R_j^{LS}$, where the superscript ^{LS} comes from Least Squares, $Q_j^{LS} = [Q_j^{LS(1)},\ Q_j^{LS(2)}]$ with $Q_j^{LS(1)} \in \mathbb{C}^{(k+n_j+p)\times(k+n_j)}$ and $Q_j^{LS(2)} \in \mathbb{C}^{(k+n_j+p)\times p}$, $R_j^{LS} = \begin{bmatrix} R_j^{LS(1)} \\ 0_{p\times(k+n_j)} \end{bmatrix} \in \mathbb{C}^{(k+n_j+p)\times(k+n_j)}$ with $R_j^{LS(1)} \in \mathbb{C}^{(k+n_j)\times(k+n_j)}$ is an upper triangular matrix, from which the reduced QR-factorization of $\underline{\mathscr{F}}_j$ is formulated as $\underline{\mathscr{F}}_j = Q_j^{LS(1)} R_j^{LS(1)}$ if $Q_j^{LS(1)}$ is considered as an orthogonal basis of $\underline{\mathscr{F}}_j$. Thus, we could still formulate Y_j in a relatively economic way as

$$Y_j = (R_j^{LS(1)})^{-1}((Q_j^{LS(1)})^H \Lambda_j) \in \mathbb{C}^{(k+n_j)\times p}, \tag{85}$$

from which we could deduce the residual of the least-squares problem described in Equation (35) as follows:

$$\begin{aligned}
\Lambda_j - \underline{\mathscr{F}}_j Y_j &= \Lambda_j - Q_j^{LS} R_j^{LS} Y_j = Q_j^{LS}\left((Q_j^{LS})^H \Lambda_j - R_j^{LS} Y_j\right), \\
&= Q_j^{LS}\left(\begin{bmatrix} (Q_j^{LS(1)})^H \\ (Q_j^{LS(2)})^H \end{bmatrix} \Lambda_j - \begin{bmatrix} R_j^{LS(1)} \\ 0_{p\times(k+n_j)} \end{bmatrix} Y_j\right), \\
&= Q_j^{LS}\left(\begin{bmatrix} 0_{(k+n_j)\times(k+n_j+p)} \\ (Q_j^{LS(2)})^H \end{bmatrix} \Lambda_j\right), \\
&= Q_j^{LS}\begin{pmatrix} 0_{(k+n_j)\times p} \\ R_j^{\ell s} \end{pmatrix},
\end{aligned}$$

where $R_j^{\ell s} = (Q_j^{LS(2)})^H \Lambda_j \in \mathbb{C}^{p\times p}$ are the last p rows of $(Q_j^{LS})^H \Lambda_j$. The SVD of scaled residual $R_j^{\ell s} D_\varepsilon$ can be written as

$$R_j^{\ell s} D_\varepsilon = U_{\ell s} \Sigma V_{\ell s}^H,$$

so that the SVD of the scaled least squares residual is

$$\left(\Lambda_j - \underline{\mathscr{F}}_j Y_j\right) D_\varepsilon = \underbrace{Q_j^{LS}\begin{pmatrix} 0_{(n_j+k)\times p} & I_{n_j+k} \\ U_{\ell s} & 0_{p\times(n_j+k)} \end{pmatrix}}_{\text{Unitary}} \begin{pmatrix} \Sigma \\ 0_{(n_j+k)\times p} \end{pmatrix} V_{\ell s}^H.$$

F Numerical results for IB-BGMRES-DR-VA

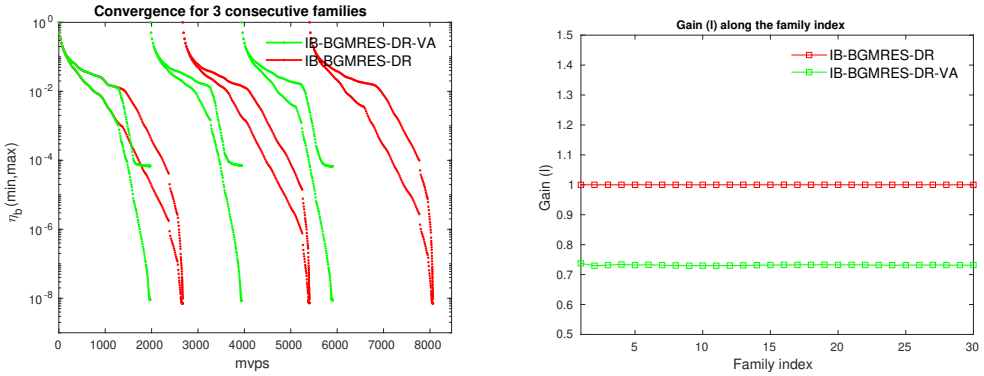

Figure 11: Comparison of IB-BGMRES-DR to IB-BGMRES-DR-VA on families built by Matrix 1 with parameters as $p = 20$, $m_d = 300$ and $k = 30$. Left: convergence histories of largest/smallest backward errors $\eta_{b^{(i)}}$ at each $mvps$ for 3 consecutive families. Right: Gain (ℓ) of IB-BGMRES-DR-VA to IB-BGMRES-DR verse family index.

Number of families	Method	$mvps$	its
3	IB-BGMRES-DR	8066	515
	IB-BGMRES-DR-VA	**5903**	**490**
30	IB-BGMRES-DR	80717	5191
	IB-BGMRES-DR-VA	**59069**	**4957**

Table 8: Numerical results of IB-BGMRES-DR and IB-BGMRES-DR-VA in terms of $mvps$ and its, where the coefficient matrix is Matrix 1 with involving parameters defined as $p = 20$, $m_d = 300$ and $k = 30$.

G Numerical results for IB-BGMRES-DR-CB

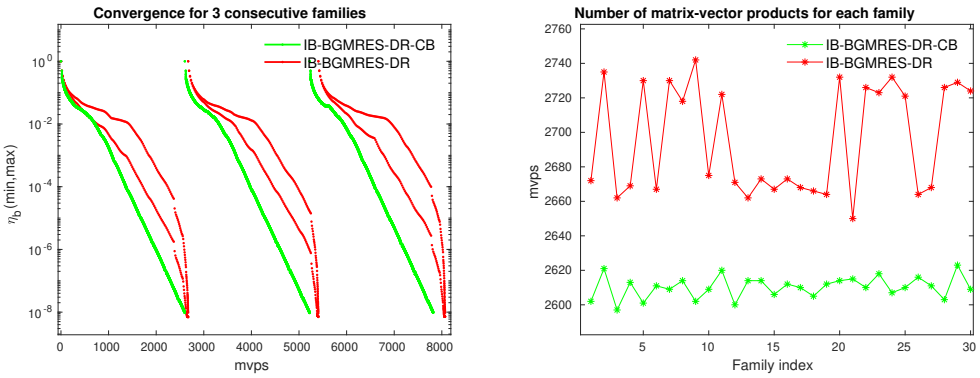

Figure 12: Comparison of IB-BGMRES-DR to IB-BGMRES-DR-CB on families constructed by Matrix 1 with parameters setting as $p^{CB} = 1$, $p = 20$, $m_d = 300$ and $k = 30$. Left: convergence histories of largest/smallest backward errors $\eta_{b^{(i)}}$ at each $mvps$ for 3 consecutive families. Right: number of consumed $mvps$ verse family index.

Number of families	Method	$mvps$	its
3	IB-BGMRES-DR	8069	**515**
	IB-BGMRES-DR-CB ($p^{CB} = 15$)	7844	561
	IB-BGMRES-DR-CB ($p^{CB} = 1$)	**7820**	7250
30	IB-BGMRES-DR	80861	**5198**
	IB-BGMRES-DR-CB ($p^{CB} = 1$)	**78308**	72608

Table 9: Numerical results of IB-BGMRES-DR, IB-BGMRES-DR-CB with parameter $p^{CB} = 1, 15$ in terms of $mvps$ and its, where the involving parameters for Matrix 1 are set to be $p = 20$, $m_d = 300$ and $k = 30$.

H Numerical results for various target accuracy

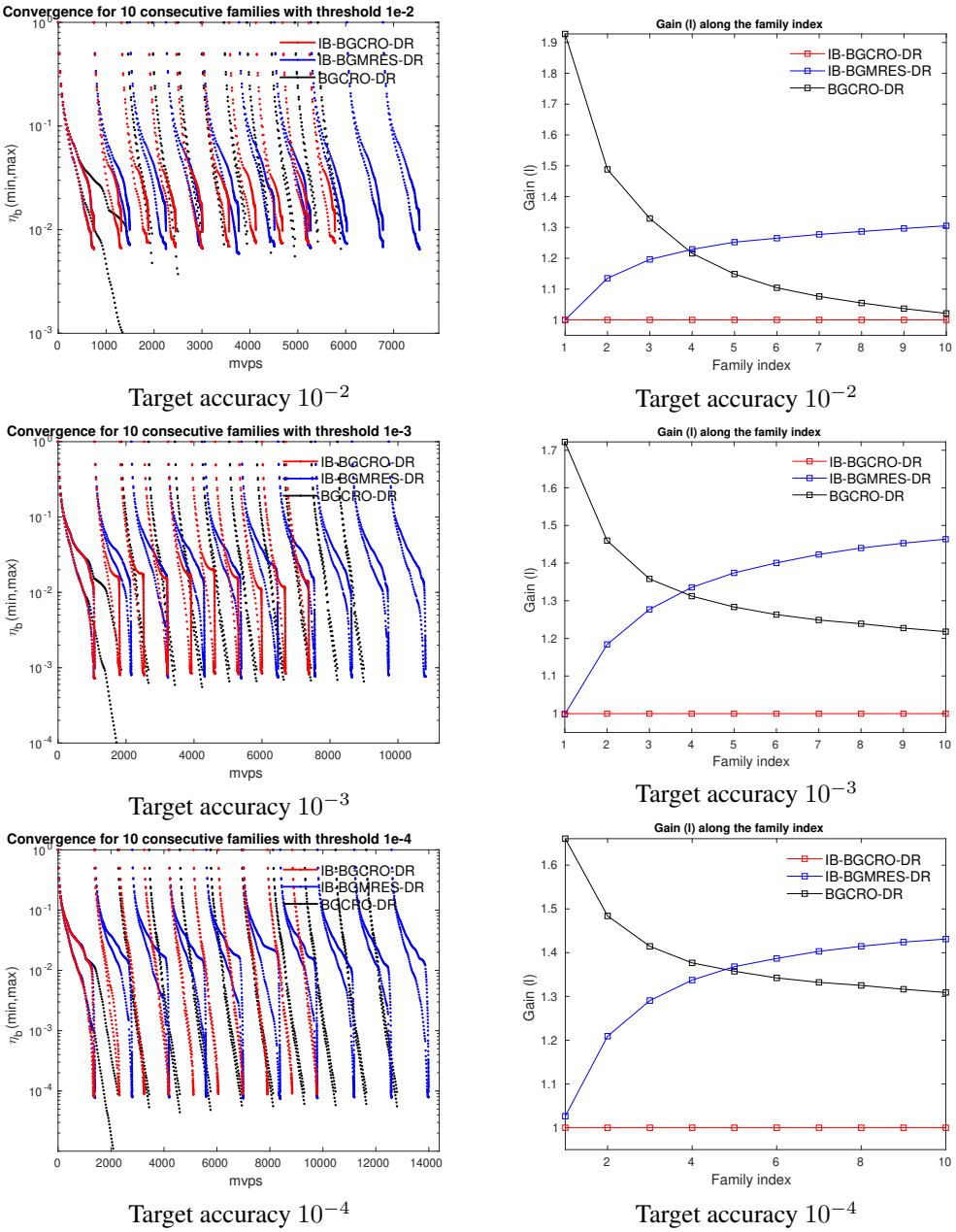

Figure 13: History of Section 5.3 for the behavior in case of different target accuracy (10^{-2}, 10^{-3} and 10^{-4}) for the families constructed by Matrix 1 with parameters setting as $p = 20$, $m_d = 300$ and $k = 30$. Left: convergence histories of IB-BGCRO-DR, BGCRO-DR and IB-BGMRES-DR on the largest/smallest backward errors $\eta_{b^{(i)}}$ at each $mvps$ for 10 consecutive families. Right: Gain (l) of the block methods with respect to IB-BGCRO-DR along family index.

I Comparison with IB-BGMRES-DR in terms of reusing information

IB-BGMRES-DR [1] is a block GMRES method that enables the deflated restarting strategy proposed by Morgan [12] for recycling spectral information at a new cycle and the inexact breakdown mechanism introduced by Robbé and Sadkane [19] for handling the issue of almost rank deficient block generated by the block Arnoldi procedure. Assume the way of approximating spectral information is the same for the IB-BGCRO-DR and IB-BGMRES-DR methods, the major difference between this two IB methods arise from their way of reusing such generated spectral information as described in Figure 14, in which the content in rectangle refers to the algorithm adopted in corresponding cycle and the directed arrow illustrates generating target spectral information at the end of the j-th $(j = 1, 2, \cdots)$ cycle (or family) and then reusing it in the subsequent $(j+1)$-th cycle (or family) for convergence acceleration. Figure 14 illustrates that unlike IB-BGCRO-DR which could reuse spectral information from the solutions of previous family and cycle, IB-BGMRES-DR can only reuse information from the previous cycle, which means IB-BGMRES-DR could solely solve each individual family of linear systems (1) separately without benefiting from information generated when solving the previous family. Therefore, IB-BGCRO-DR and IB-BGMRES-DR could be mathematically equivalent to each other under some conditions (like using the same way to approximate eigen-information) as the relationship between (block) GCRO-DR and (block) GMRES-DR when solving single family in Equation (1), while the performance of the former one overs the later one when solving subsequent related-sequence families thanks to its ability of recycling spectral information between families as described in top red parts of Figure 14, and which has been verified by the numerical results shown in Section 5.3.

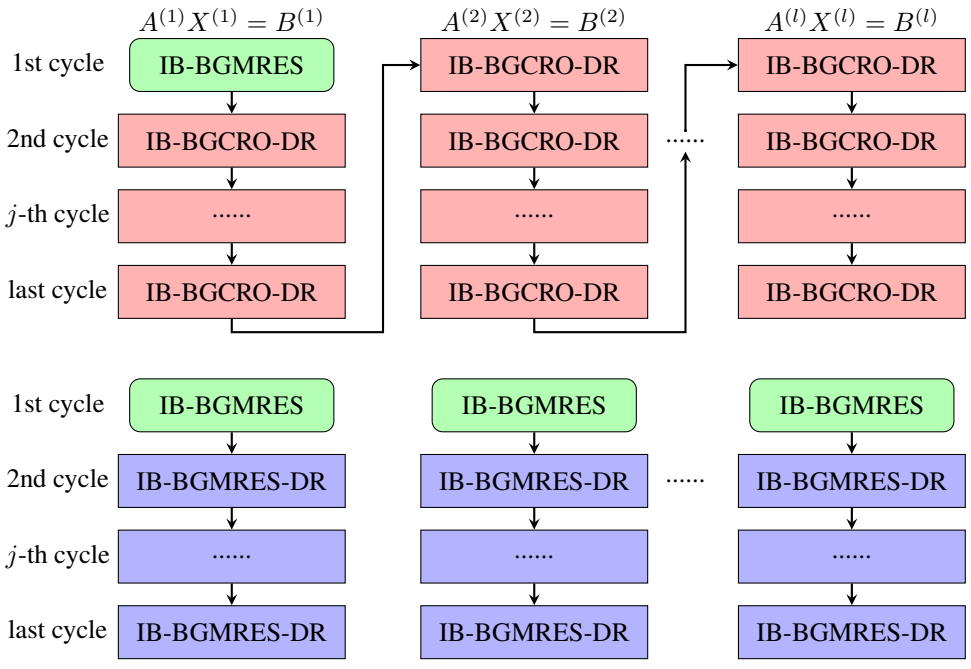

Figure 14: Flowchart of reusing spectral information in the IB-BGCRO-DR (top) and IB-BGMRES-DR (bottom) algorithms

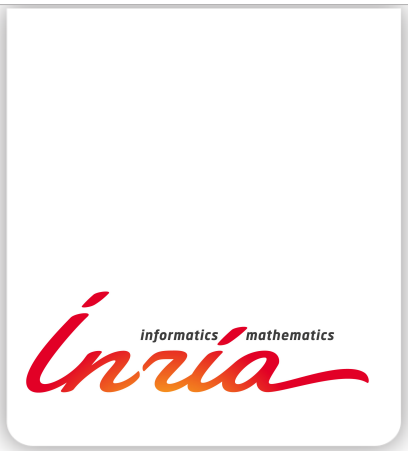

RESEARCH CENTRE
BORDEAUX – SUD-OUEST

200 avenue de la Vieille Tour
33405 Talence Cedex

Publisher
Inria
Domaine de Voluceau - Rocquencourt
BP 105 - 78153 Le Chesnay Cedex
inria.fr

ISSN 0249-6399